Quaternary Science Reviews xxx (2014) 1–18

Contents lists available at ScienceDirect

Quaternary Science Reviews

journal homepage: www.elsevier.com/locate/quascirev

Coseismic vs. climatic factors in the record of relative sea level changes: an example from the Last Interglacials in SE Spain

T. Bardají [a, *], A. Cabero [b], J. Lario [b], C. Zazo [c], P.G. Silva [d], J.L. Goy [e], C.J. Dabrio [f]

[a] U.D. Geología, Dpto. Geología, Geografía y Medio Ambiente, Universidad de Alcalá, 28871 Alcalá de Henares, Madrid, Spain
[b] Facultad de Ciencias, UNED, 28040 Madrid, Spain
[c] Dpto. Geología, Museo Nacional CC, Naturales, CSIC, 28006 Madrid, Spain
[d] Dpto. Geología, Universidad de Salamanca, EPTS de Avila, 05003 Ávila, Spain
[e] Dpto. Geología, Facultad de Ciencias, Universidad de Salamanca, 37008 Salamanca, Spain
[f] Dpto. Estratigrafía, Facultad de CC. Geológicas, UCM, 28040 Madrid, Spain

ARTICLE INFO

Article history:
Received 30 May 2014
Received in revised form
3 October 2014
Accepted 9 October 2014
Available online xxx

Keywords:
Betic Cordillera
Marine terraces
Coastal uplift
Geomorphologic analysis

ABSTRACT

Trying to decipher how paleoseismic activity has influenced the altitudinal disposition of interglacial deposits is one of the main challenges to be confronted before quantifying relative sea-level changes between consecutive highstands. At the same time, identifying paleoseismic features in an area with low instrumental seismic activity can complement the seismic record, thereby contributing to better seismic hazard knowledge. In this regard, Cope Basin (SE Spain) meets all the requirements necessary for these kinds of analysis, firstly on account of its excellent outcrop conditions and secondly, because its sea level record is undoubtedly conditioned by both factors: climatically driven changes and local and regional seismotectonics.

The morpho-sedimentary sequence presented in this paper provides evidence from three different highstands: two littoral sedimentary units separated by terrestrial deposits and affected by liquefaction (paleoseismic activity), and a younger paleo-cliff and its associated wave-cut platform carved into those sedimentary units. This wave-cut platform now tilted and folded, reaches heights ranging from 0 to +8 m, which has been interpreted as a consequence of cosesimic effect. The age of this wave-cut platform (Last Interglacial or Holocene) supports uplift rate estimations of from 0.016 to 0.15 mm/yr since the Last Interglacial/Holocene. Active deformation observed on Pleistocene–Holocene sea-level geomarkers can not only furnish useful information about seismic activity within the major structure of the Aguilas Arc, but also offer new insight into the Cope Basin's geodynamic model.

1. Introduction

The presence of sea-level geomarkers makes coastal settings areas of prime interest for reconstructing the history of climatically driven relative sea-level changes. However, in tectonically active regions, the seismotectonic component can alter the position of sea-level geomarkers significantly, thereby upsetting this paleo-sea-level history. It is therefore important know to what extent there has been seismotectonic activity before fully understanding the nature of the recorded relative sea-level changes.

Tectonic activity in South-eastern Spain is a direct consequence of its position within the African–Eurasian convergence zone that extends the whole length of the Mediterranean Sea. There is great variation in this scenario from the eastern to the western Mediterranean, with convergence rates varying from a few centimetres per year in a NE direction (Eastern Mediterranean) to a few millimetres per year in a NNW direction (Western Mediterranean) (Morelli and Barrier, 2004), as also borne out by differing levels of seismicity from the eastern to the western Mediterranean.

In South-eastern Spain these convergence processes lead to the development of two major tectonic structures: the Eastern Betics Left Lateral Shear Zone, (Ott d'Estevou and Montenat, 1985; Montenat et al., 1987; Larouziere et al., 1988; Silva et al., 1993) and the Aguilas Arc (Coppier et al., 1989; Griveaud, 1989), which can be defined as a differentially up-thrusted cortical structure characterized by a large-scale bending and indentation of the upper crust (Coppier et al., 1989; Griveaud, 1989; Silva et al., 1993), (Fig. 1a). Seismic activity throughout the area is closely related to

* Corresponding author.
E-mail address: teresa.bardaji@uah.es (T. Bardají).

http://dx.doi.org/10.1016/j.quascirev.2014.10.005
0277-3791/

the recent evolution of these major structures and is higher in the periphery of the Arc, where there is a concentration of compressive stress (Silva et al., 1993) (Fig. 1b).

Worldwide data about the effects of earthquakes on coastal areas focus predominantly on regional uplift/subsidence in relation to high magnitude megathrust earthquakes (some examples in Plafker, 1969; Nelson et al., 1996; Ortlieb et al., 1996a,b; Meltzner et al., 2006; Ozawa et al., 2011; Melnick et al., 2012). However, less information is available for areas where no subsidence zones develop and seismicity focuses mainly on active late Quaternary faults and folds, such as western Mediterranean areas. Some examples have been recently published for coseismal surface deformations (faults, flexures and uplift) affecting Last Interglacial coastal sediments and archaeological–historical remains in Tunisia (Bahrouni et al., 2014), Italy (Ferranti et al., 2007; Cuci and Tertuliani, 2010) or Algeria (Maouche et al., 2011).

The reconstruction of sea-level changes during the most recent and present interglacials in SE Spain on the one hand, and the role of regional neotectonics in the present distribution of marine terraces on the other, have been approached by different authors (e.g. Goy et al., 1993; Zazo et al., 2003; Rodríguez-Vidal et al., 2004; Hearty et al., 2007; Bardají et al., 2009; Dorale et al., 2010; Dabrio et al., 2011; Tuccimei et al., 2012; etc). Zazo et al. (2003) reviewed the raised marine terraces along the Spanish coasts, analysing their different disposition with regard to the tectonic domain. Different tectonic scenarios form strong uplift in the Gibraltar area, subsidence areas in the Mar Menor region (SE Iberian Peninsula), cause different arrangements of the marine terraces, from staircase and offlapping in uplifted areas, to overlapping and onlapping in subsiding areas.

However, the differentiation between climatic (*eustatic*) and seismotectonic components in the record of relative sea-level changes requires precise estimates for sea level during the interglacial under consideration, estimates which to date vary greatly. Sea level during MIS 5e has been studied worldwide and more is known about it than the sea level for all other interglacials. Nevertheless, there is still much debate about the height reached by sea level during this interglacial even in tectonically stable areas. Several works (Siddall et al., 2006; Hearty et al., 2007; Kopp et al., 2009; Pedoja et al., 2011; Dutton and Lambeck, 2012) have tried to answer this question, but there is still no general agreement about sea level during MIS 5e. Siddall et al. (2006) consider that sea level for MIS 5e generally lies within the range of +2–+4 m, as reported by Stirling et al. (1998) in Western Australia. This fits with the range of 0–+6 m suggested by Schellmann and Radtke (2004) in Barbados. Hearty et al. (2007) present a MIS 5e characterized by at least three sea-level highstands (+2–+3 m, +3–+4 m, +6–+9 m). Kopp et al. (2009) lay great emphasis on the differences between local and global sea levels as an impediment for accurately reconstructing past sea levels. Nonetheless, bearing that in mind, the same authors give a 95% probability for a global sea-level 6.6 m higher than today during MIS 5e, 67% for a sea-level 8.0 m higher and 33% (unlikely) for a sea-level position 9.4 m higher that today. Pedoja et al. (2011) compiled more than 800 published references worldwide that point to a mean elevation of +28 m for MIS 5e, which they interpret as an average global uplift of shorelines. Finally, Dutton and Lambeck (2012) analyse the elevation and age of MIS 5e at 16 sites around the world with a view to quantifying the contribution from the Greenland and Antarctic ice sheets. The sea-level heights they consider are between the same values given by the preceding authors, namely, +4–+6 m, or even +9 m. However, they believe that sea level during MIS 5e could vary from one location to another, depending on its distance from former and subsequent ice sheets, as well as its response to isostatic adjustments to ice and water loading.

As far as seismicity is concerned, we analyse not only its role played in the unevenness of past sea-level indicators but also the importance of identifying paleoseismic evidence in areas with low instrumental seismicity. These paleoseismic features become an important tool for enhancing the seismic record in an area where low recurrence, destructive earthquakes can occur. In this sense, the distortions observed in Pleistocene–Holocene sea-level indicators provide useful information about paleoseismic activity within the major structure of the Aguilas Arc, while also offering new insight into the geodynamic model for the Cope Basin (Bardají et al., 2010).

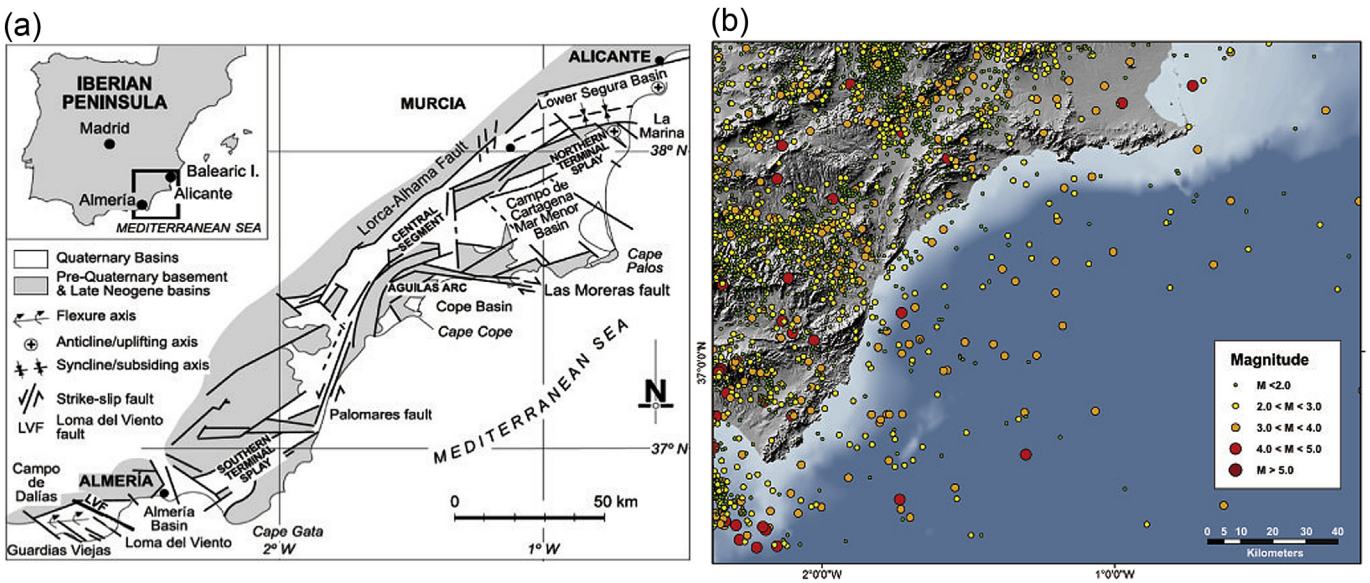

Fig. 1. Location map; (a) structural and (b) seismic framework of the Eastern Betics Shear zone and Aguilas Arc. (Mod. from Silva et al., 1993; seismic data from IGN database browser, 2014).

Please cite this article in press as: Bardají, T., et al., Coseismic vs. climatic factors in the record of relative sea level changes: an example from the Last Interglacials in SE Spain, Quaternary Science Reviews (2014), http://dx.doi.org/10.1016/j.quascirev.2014.10.005

2. Study site

2.1. Seismotectonic framework

The area's regional geodynamics is governed by the major left lateral transcurrent zone (Fig. 1), known as the Eastern Betics Shear Zone (EBSZ) (Ott d'Estevou and Montenat, 1985; Montenat et al., 1987; Larouziere et al., 1988; Silva et al., 1993), generated in response to the indentation process which triggered the development of the Aguilas Arc (Coppier et al., 1989) from the Middle Miocene until the Quaternary (Silva et al., 1993). This structure evolved under a changing stress field that rotated from N170E to N150E during the Late Pliocene (Montenat et al., 1987) to N150E to N170E from the Early–Middle Pleistocene (Somoza, 1989; Goy et al., 1990; Silva et al., 1993), causing changes in fault kinematics and thus in the location and geometry of the sedimentary zones and bounding tectonic ranges (Silva et al., 1993).

Stronger seismic activity in the area (Fig. 1) is clearly concentrated along those faults within the EBSZ which are oriented perpendicular or oblique to the main stress field. This is the case of the Lorca – Alhama, Carrascoy, Lower Segura or Crevillente faults (Silva, 1994; Martínez-Díaz, 2002; Martínez-Díaz et al., 2011). These ENE–WSW to E–W faults produced instrumental earthquakes of 5.2 Mw and historical ones of estimated magnitudes ranging from 6.2 to 6.9 Mw (Martínez-Díaz et al., 2011; Alfaro et al., 2012). Active faults parallel to the direction of the regional stress field yield higher slip-rates but very low seismic activity, as is the case of the Palomares fault which has recorded a maximum accumulated left-lateral offset of 30 km (N–S) since the early Pleistocene (Bousquet, 1979; Weijermars, 1987). This fault is of significance because it constitutes the outer western border of the indented crustal block of the Aguilas Arc and the aforementioned accumulated offset is mainly derived from this process (Coppier et al., 1989). However, instrumental seismicity in this fault zone is very low ($\leq$3.0 Mw), even in the northern bend of the indenter (Silva et al., 1993) formed by the N120E Las Moreras Range fault-zone (Fig. 1a). Present N–S compressive stresses (N170E) are mainly accumulated in the northern terminal splay of the EBSZ, delimited by the Crevillente and Lower-Segura Faults. This last is a blind thrust-fault of overall E–W orientation, displaced by transversal N120E dextral faults (Fig. 1a), and is the seismic origin of the aforementioned strong historical events (6.2–6.9 Mw). Its seismic activity throughout the entire Holocene is attested by the occurrence of multiple "seismite layers" (Paleo-liquefaction features) in the sedimentary record of the adjacent Lower-Segura Basin (Alfaro et al., 2012).

In the Aguilas Arc, from the Pliocene onwards individual NE–SW (South) to ENE–WNW (North) thrust-faults controlled the location and geometry of small littoral sedimentary basins (Águilas, Cope and Ramonete) within the indented crustal block (Giménez et al., 2000; Bardají et al., 2010). These structures are noticeably rotated and bent towards the East as a consequence of the differential northwards displacement of the indenter during the entire Plio-Quaternary. This northwards displacement gave rise in turn to differential uplift and faulting of outcropping Early to Late Pleistocene littoral sedimentary sequences (Bardají, 1999), as well as to apparent folding linked to blind-thrust faults on the Plio-Quaternary series. However, the zone's seismic record is scant, with few low magnitude instrumental earthquakes ($\leq$4.0 Mw; Fig. 1b) and only two historic earthquakes (AD 1596 and AD 1882), whose macroseismic epicentre was in the locality of Águilas and which registered maximum intensities of IV–V (Mezcua, 1982; IGN, 2014). Geodetic studies in this zone indicate that in spite of this low seismic activity, the internal E–W to ENE–WSW thrusts of the Águilas Arc yield the highest uplift-rates in the Eastern Betic Cordillera, with maximum values of 0.95 ± 0.2 mm (Giménez et al., 2000). These authors used levelling-lines from 1934 to 1976 to detect a positive asymmetric anomaly of 40 ± 8 mm south of Águilas.

2.2. Structure and sedimentary filling of the Cope Basin

The Águilas Arc inner basins opened during the Early Pliocene in response to the differential uplift of the main thrust-sheets (Málaguide, Alpujárride and Nevado-Filabride Betic internal units) involved in the indented Águilas block within the regional compressive scenario of the EBSZ. N120E and N60E faults led to the opening of the Cope Basin (Bardají, 1999; Silva et al., 2003), where data from boreholes indicate that no marine sedimentary materials were deposited during pre-Pliocene times (Bardají, 1999; Bardají et al., 2010). The first Pliocene series comprises submarine basalts and fine-grained marine blue clayey-silts (>100 m thick), which evolve upwards to littoral sequences of sandy-silts and gravels to the eventual deposition of Plio-Quaternary marls and dominantly yellow fossiliferous calcarenites (c. 50 m thick). Borehole data gathered by Bardají (1999) indicate vertical displacements of c. 50–100 m and significant thickness changes (±45 m) in these two last Pliocene series over horizontal distances of 500–1500 m, probably as a result of synsedimentary faulting.

This tectonic scenario resembles the Pleistocene to Holocene deformation recorded in the terminal splay of EBSZ (Lower Segura blind-fault), as described by Alfaro et al. (2012). In the case of the Águilas Arc basins, especially in the Cope Basin, this scenario occurred earlier, during Plio-Pleistocene times, since the evolution of the entire EBSZ implies a northwards propagation of thrust-faulting and the subsequent progressive generation of basins and bounding anticline-like reliefs, such as the Carrascoy or La Tercia ranges and Lower Segura anticline-ranges (Silva et al., 1993). In the Cope Basin, N–S shortening produced by blind-faults at depth is partially accommodated by the generation of more recent NE–SW (N120E) strike-slip oblique faults, as presently occur in the Lower Segura Fault (Alfaro et al., 2012). This set of faults governed not only the sedimentation and relief patterns during the Middle–Late Pleistocene within the Cope Basin (Bardají et al., 2010), but also the spatial and altitudinal distribution of Pleistocene marine and terrestrial units. The two most prominent tectonic structures of the basin define its northern compressive margin as in contact with the Betic metamorphic substratum, La Galera (NE–SW) and La Panadera (E–W) faults (Fig. 2). These are strike-slip reverse faults forming a narrow push-up structure in which basin filling materials and the metamorphic substratum are complexly folded, faulted and uplifted.

The yellow fossiliferous calcarenites are deformed by NE–SW to ENE–WSW large folds of hectometric wavelength and metric amplitude with low dip (<15°). In some cases the anticlines give place to small-elongated mesas in which asymmetric fold limbs occur. These materials are unconformably overlain by a well-cemented NW–NE offlapping Pleistocene sedimentary sequences where shallow marine and coastal sediments alternate with sub-aerial alluvial fans (Bardají et al., 1986; Goy et al., 1987; Dabrio et al., 1991; Bardají, 1999; Zazo et al., 1998, 2003, 2013). The arrangement of this sedimentary sequence is mainly conditioned by the more recent N120E fault system, but differential inland uplift along the Quaternary resulted in a seawards-offlapping (NW-SE) arrangement of marine and terrestrial morphosedimentary units (Fig. 3).

The whole sedimentary sequence, composed of up to ten marine units, has been entirely attributed to the Pleistocene. This chronology is supported by paleomagnetic, paleontologic and regional field data. Paleomagnetic results (Bardají et al., 1995) show two inversions in polarity. The first one, from normal to reverse polarity,

Please cite this article in press as: Bardají, T., et al., Coseismic vs. climatic factors in the record of relative sea level changes: an example from the Last Interglacials in SE Spain, Quaternary Science Reviews (2014), http://dx.doi.org/10.1016/j.quascirev.2014.10.005

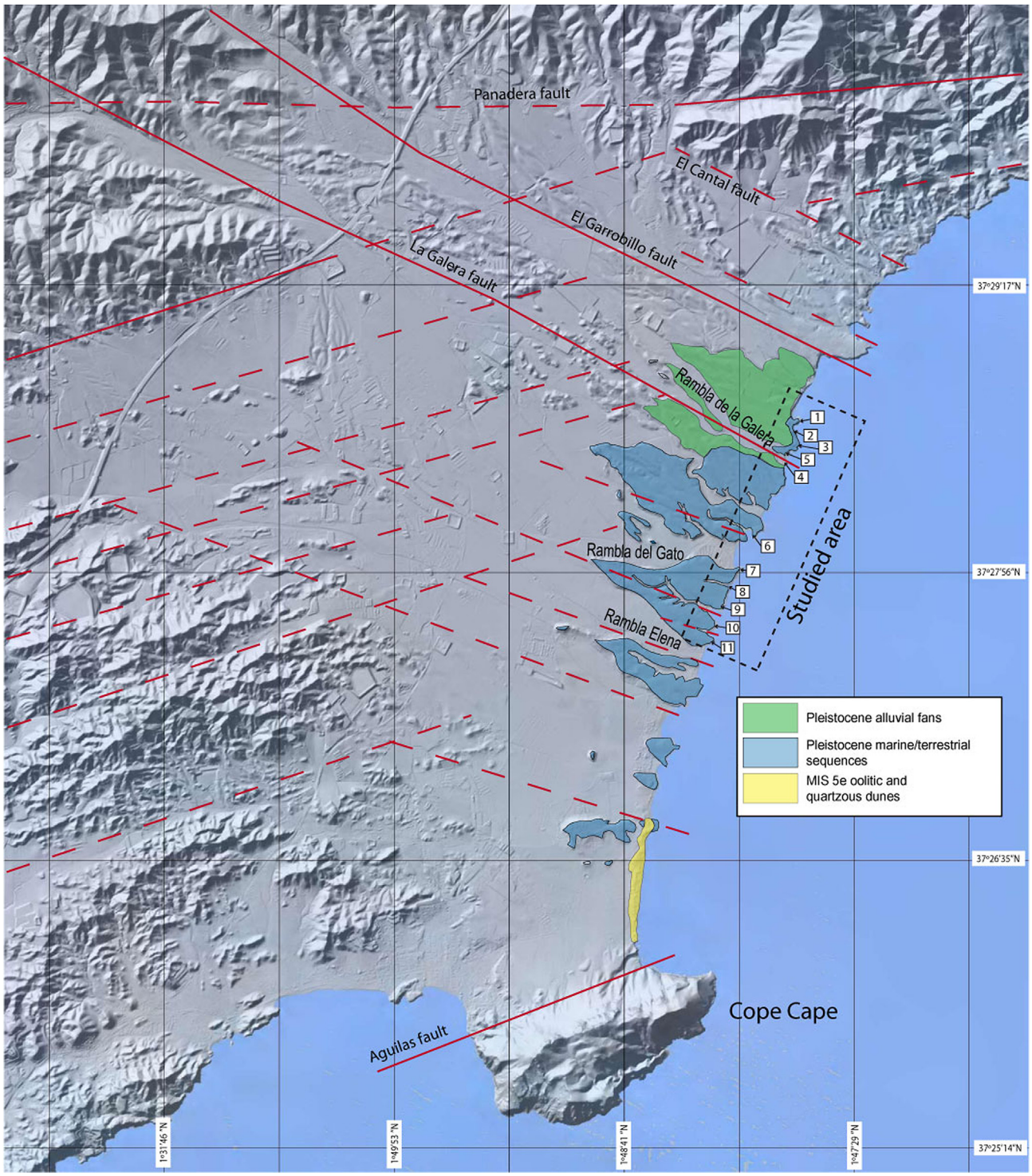

Fig. 2. Cope Basin, main faults and monocline delta-shaped reliefs. 1–11: location of studied sections.

has been interpreted as the upper Matuyama–Olduvai boundary and occurs in the upper part of the underlying yellow calcarenites unit. The second paleomagnetic reversal (reverse to normal polarity) is recorded within the fourth morphosedimentary marine unit, and has been interpreted as the Matuyama–Brunhes boundary (ca 0.7 Myr).

The preserved sequence is capping the delta-shaped reliefs which, descending smoothly to the sea, characterize this basin (Fig. 2). The development of these delta-shaped reliefs is controlled by the more recent N120E fault system. They may be considered separate structural blocks, varying noticeably in altitude due to faulting and ongoing differential folding throughout the Pleistocene. Main features are small rocky cliffs (3–8 m high) with some sparse pocket beaches or coves usually located at the mouth of the active "ramblas" (wadi-like ephemeral rivers) controlled by the N120E faults (Fig. 2).

Please cite this article in press as: Bardají, T., et al., Coseismic vs. climatic factors in the record of relative sea level changes: an example from the Last Interglacials in SE Spain, Quaternary Science Reviews (2014), http://dx.doi.org/10.1016/j.quascirev.2014.10.005

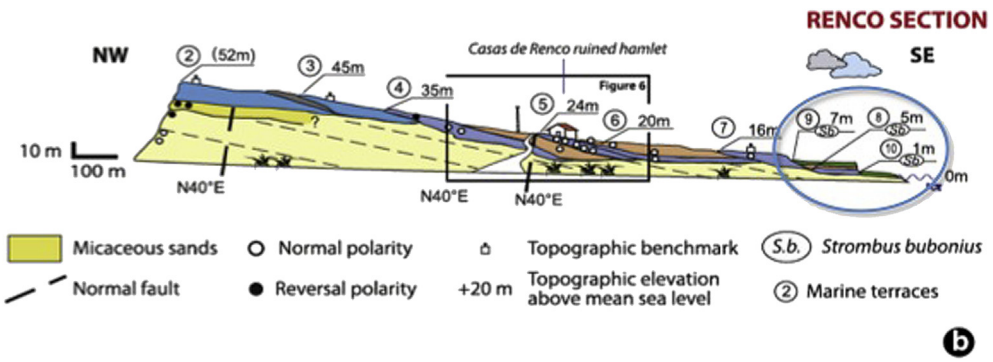

Fig. 3. Renco section: General sedimentary sequence (mod. from Bardají et al., 1986).

The three younger units present a staircase arrangement in the general offlapping sequence, with the youngest further staircased into the two older units. The youngest is only barely visible in a single outcrop at +0.5 m, but the two older ones are easy to trace along the basin and have been attributed to MIS 7 and MIS 5 on the basis of their fauna (*Strombus bubonius*) and their relation with the MIS 5e sedimentary oolitic facies (Bardají et al., 2009).

These two most recent sedimentary units (MIS 7–MIS 5) are exposed along the coast's rocky cliffs to the seaward end of the above-mentioned delta-shaped relieves. Their arrangement depends on their location but it usually develops on top of a former wave-cut platform ("a" in Fig. 4) carved into Plio-Pleistocene yellow calcarenites (Unit A in Fig. 4) and staircased into the older sequence of Pleistocene marine terraces (8, 9, 10 in Fig. 3). This sedimentary sequence is composed of three "key" units (Units B, C and D in Fig. 4) that can be followed along the shore and are cut by a younger wave-cut bench ("b" in Fig. 4).

As the 3D arrangement of these "key" units varies among the different structural blocks throughout the basin, if analysed in detail it may provide information on the driving factors behind the observed arrangement and consequently help to unravel the interplay in this basis between tectonics and relative sea-level history since MIS 7.

2.3. Description of main sedimentary units

The sedimentary units composing the aforementioned synthetic section present some characteristics that vary along the coast depending on their location. In what follows, a description is given of each unit and their sedimentary and petrographic characteristics:

Unit A. Plio-Pleistocene yellow calcarenites that constitute the basis of the studied sequence. This cemented unit is characterized by its high content of rhodoliths, ostreids and *Clypeaster echinoid* remains. Dissolution of aragonitic mollusc fragments and moulds are visible in thin section (Fig. 5).

Unit B. Yellow fine-bedded (dm scale) calcarenites (Fig. 5) alternating with gravel levels (both coastal and continental origin) of variable thickness. General decrease in grain-size from NE (coarser) to SW (finer) attest a NE–SW longshore drift at the moment of deposition. Sediments contain quartz grains, metamorphic rock fragments and bioclasts, including a high amount of calcareous algae fragments and foraminifera (some of them reworked from Unit A). Calcite cement and replacement in some bivalves and gastropod shell fragments visible to microscope. Rhodoliths, ostreids, barnacles, echinoids, and *Glycymeris* fragments are preserved. Karstification and small solution pipes are present at the top of the unit in some parts of the studied transect. Particular features displayed in this unit are:

a. At least two different sub-units, with different progradation directions
b. Sedimentary structures characterizing foreshore–shoreface environments.

Unit C. Intermediate terrestrial unit (Fig. 6) strongly erosive into Unit B and even into underlying Plio-Pleistocene yellow calcarenites. Channel morphologies oriented NW–N/SE–S are observed along the studied transect. The unit presents two different facies patterns:

a. Purple/grey gravels including fragments of schists, phyllites, slates, dolomites and quartz, embedded in a fine-grain size matrix. In thin section, matrix is composed of dolomitic mudstone, with fine-grained dolomite crystals. No bioclasts or clay minerals are present.
b. Fine grained laminated purple dolomitic muds (fine sands and silts) with no clay minerals. Convolute laminations usually occur in this facies. Several coastal sandy levels (with shells and bioclasts) appear at the top of the unit, also displaying soft sediment deformation features.

Unit D. Grey conglomerate of coastal origin (Fig. 7) characterized by dominating presence of rounded quartz pebbles (cm scale),

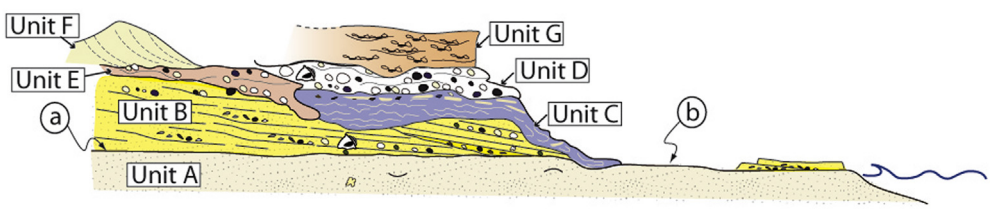

Fig. 4. Synthetic section of studied sedimentary sequence. Unit A: Plio-Pleistocene yellow calcarenites; Unit B: MIS 7 fine bedded beach calcarenites; Unit C. Purple continental gravels and muds; Unit D: MIS 5 quartzous grey gravel beach conglomerate; Unit E: Reddish conglomerate; Unit F: Quartzous aeolian dune; Unit G: Alluvial fan reddish gravels; a: pre-MIS 7 wave cut platform; b: post-MIS 5 wave cut bench (full explanation in Section 2.3). (For interpretation of the references to colour in this figure legend, the reader is referred to the web version of this article.)

Please cite this article in press as: Bardají, T., et al., Coseismic vs. climatic factors in the record of relative sea level changes: an example from the Last Interglacials in SE Spain, Quaternary Science Reviews (2014), http://dx.doi.org/10.1016/j.quascirev.2014.10.005

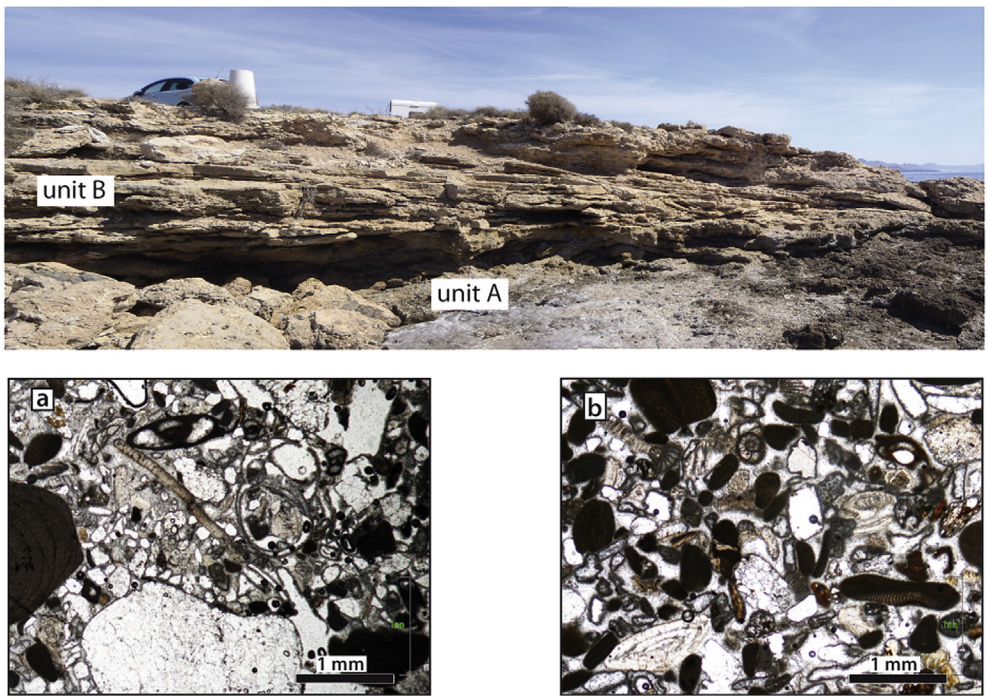

Fig. 5. Field image and microphotographs of Units A (a) and B (b) at Point 11.

cobbles and boulders. Faunal content corresponds mainly to *Glycymeris* and *Ostrea*, with a few individuals of *S. bubonius*, *Thais haemastoma* and *Conus* sp. Particular features displayed in this unit are:

a. Two different sub-units separated by terrestrial gravels have been identified in most of the outcrops, and a third one only observed in some parts of the studied transect.
b. Older sub-units present highly cemented conglomerates and calcarenites corresponding to shoreface–foreshore environments. Faunal remains include molluscs, rhodolites, foraminifera, echinoids, barnacles and bryozoa fragments.
c. Younger sub-unit presents slightly cemented conglomerates and sandstones corresponding to foreshore–backshore and dune deposits. It contains more siliciclastic sediments and fewer shell fragments.

Unit E. Conglomerate with rounded quartz pebbles, similar to those from marine Unit D but with reddish clayey matrix. Locally, it covers terrestrial deposits of Unit C. In the southern zone it underlies Last Interglacial quartzous dune (F).

Unit F. Quartzous aeolian dune with some reworked oolites. These dunes and the oolitic ones only outcrop in the southern part of the basin. Oolitic dunes characterize the peak of MIS 5e in the Spanish Mediterranean (Zazo et al., 2003; Bardají et al., 2009).

Unit G. Reddish sand, silts and gravels from lowstand alluvial fan systems overlying the sequence in the northern sector (points

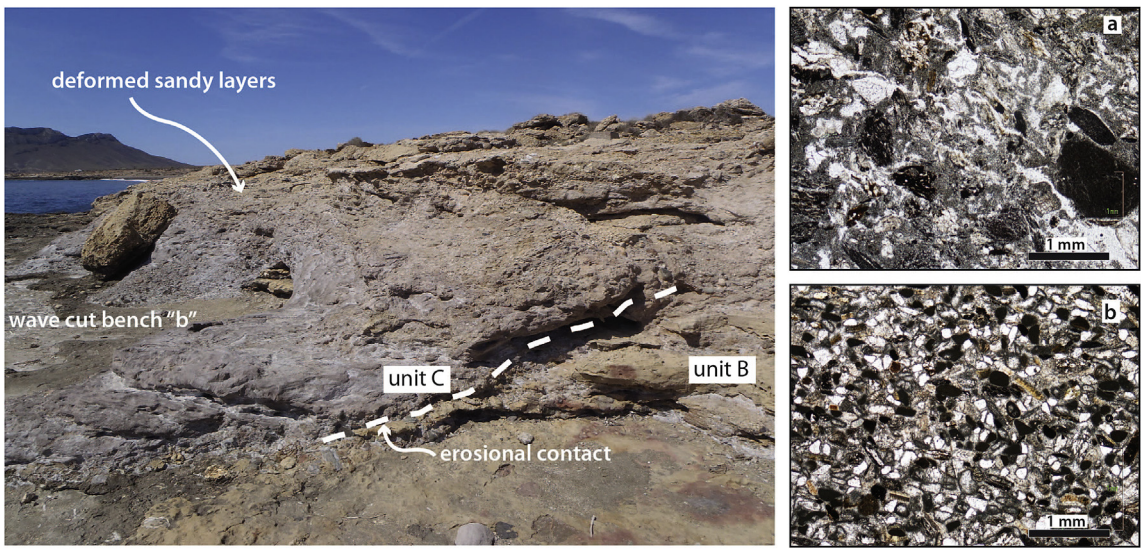

Fig. 6. Field image of Unit C at Point 11 (left); (a) Microphotograph of the matrix of the purple/grey gravels of Unit C, (b) Microphotograph of sandy beach levels at the top of Unit C.

Please cite this article in press as: Bardají, T., et al., Coseismic vs. climatic factors in the record of relative sea level changes: an example from the Last Interglacials in SE Spain, Quaternary Science Reviews (2014), http://dx.doi.org/10.1016/j.quascirev.2014.10.005

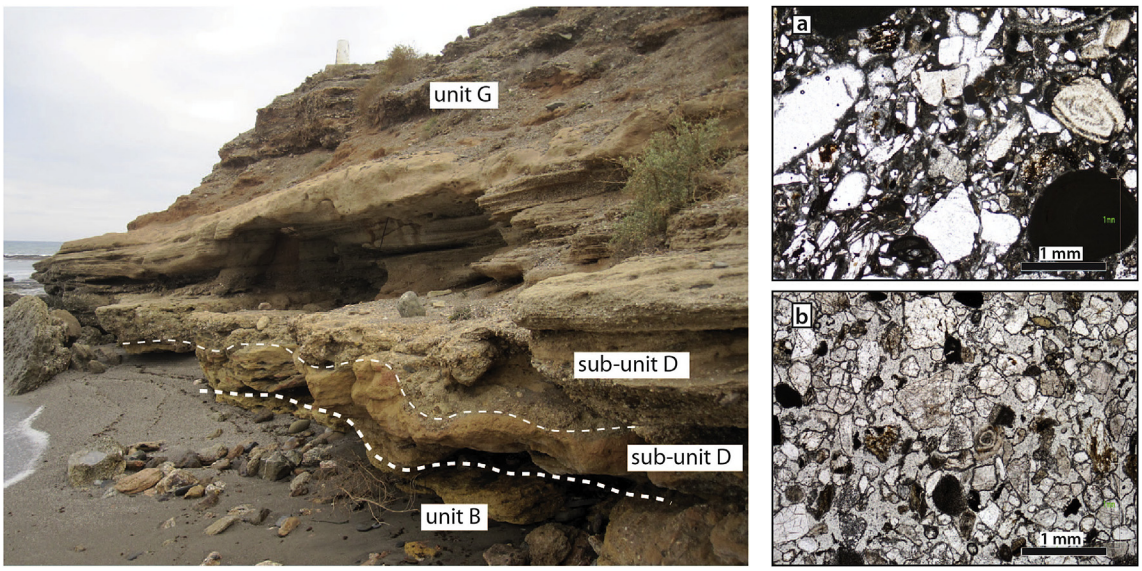

Fig. 7. Field image of Unit D (left) at Point 4; (a) Microphotograph of conglomerates of Unit D; (b) Microphotograph of less cemented sandstones corresponding to the younger sub-unit D.

2–4). Spatial distribution of these deposits as well as the age of underlying marine unit (MIS 5) point to a probable Last Glacial age for this unit.

Units E, F and G are not widespread throughout the studied sequences.

3. Methods

Geomorphologic and sedimentary facies analyses, together with petrographic microscopic determinations, have been used for the study and description of the marine and terrestrial units of the above-mentioned sedimentary type sequence. Eleven sections were described in detail along the coast (See Fig. 2 for location). These points were selected according to the following criteria: they lie in different structural blocks, the "key" sedimentary units are well preserved, the wave cut bench "b" is easily identifiable, and they bear paleoseismic evidences.

3.1. Geo-markers of sea-level position

Several geological indicators of sea level were identified and its height determined with a GPS-Altimeter Garmin Monterra at the studied points (see Fig. 2 for location). This is a barometric altimeter that needs to be calibrated every two or three hours to counter the effect of atmospheric pressure changes. Each altitudinal measurement was taken up to three or four times; the most frequently recorded was taken as good. All measurements were compared with the detailed topographic map (Sc. 1:2500) and, later, with altitudinal data from the Murcia Region Spatial Data Service (IDERM, 2014). As the accuracy of these data is in the range of 0.5–1 m and since this accuracy is the same for all the measurements, we consider them reliable enough to be taken as benchmarks for altitudinal change between the studied points. In addition, all the topographic elevations indicated in the figures were measured with respect to the high watermark, a very reliable datum in these almost-tideless coasts, where astronomical tidal ranges do not exceed 0.25 m.

As for highstands, altitude corresponds to the highest elevation of the foreshore–shoreface facies transition (the plunge-step). In the case of the marine terrace, the elevation is that of the inner edge of the terrace marked by a small, usually somewhat degraded, cliff (Dabrio et al., 2011).

1. *Inner edge of the marine terrace* (a in Fig. 8). This corresponds to the maximum altitude where each sedimentary unit outcrops and represents the maximum point reached by the sea, which in some cases may be identified by a greater accumulation of boulders, the probable result of storm events and not to be taken as the mean sea level during deposition. The altitude of this inner edge with respect to the mean sea level depends on slope, grain size, wave characteristics and storminess, among other factors; but in this basin this difference in altitude must be around 1–1.5 m. This datum mainly derives from the upper sedimentary Unit D because Unit B is usually covered by overlying Units C and D, and only in a few cases were we able to measure this maximum transgressive for Unit B as well.
2. *Plunge step* (c in Fig. 8). This sedimentary structure marks the limit between the foreshore and shoreface, indicating precisely the point where the swash-backwash process starts on the foreshore. This is a very precise geological marker since it can be considered to represent 0 m in an almost tideless coast (Dabrio et al., 1985, 2011). Unfortunately, it was not possible to identify it in every sedimentary unit, so the sparse measurements could not be used in this work.
3. *Shoreline angle of post-MIS 5 wave cut bench* ("b", in Fig. 4; b in Fig. 8). In a rocky coast, the shoreline angle is the boundary between the cliff and the wave cut bench/platform in front of it; in some cases a notch develops at this angle. It marks the maximum reach of wave action, and although in this coastal setting it can have an error of ±0.5 m, it is considered to be a reliable indicator of 0 m level. This erosional feature represents a younger, steady and long-lasting sea-level position and cuts into the whole sedimentary sequence. This wave cut bench-paleocliff coincides at some points with the former wave cut platform "a" (over the yellow calcarenites unit), or below it; in other cases it is carved into sedimentary Unit A or sedimentary Unit B. Its altitude varies dramatically among the different structural blocks, reaching heights of between 0 and 8 m.

Please cite this article in press as: Bardají, T., et al., Coseismic vs. climatic factors in the record of relative sea level changes: an example from the Last Interglacials in SE Spain, Quaternary Science Reviews (2014), http://dx.doi.org/10.1016/j.quascirev.2014.10.005

Fig. 8. Examples of the sea level geological markers described in this work. a: Inner edge of Unit B (point 8); b: Shoreline angle of wave-cut bench b (point 1); c: plunge step in Unit D (point 6).

3.2. Altitudinal analysis

In order to determine the causes of the relative sea-level changes we plotted the heights measured for the sea level geomarkers described above, specially the height of the inner edge of Unit D and the height of the wave-cut bench "b", since they represent two successive sea-level highstands and thus record an important basin-wide relative sea level drop. Comparison of these two altitudes for the studied points would help us identify the main driving factor for this sea-level drop.

The working hypothesis was that if this sea-level drop were climatically driven, the difference in altitude between these two markers should be uniform along the coast, regardless of their present-day altitude; but if the difference in altitude varies among the studied structural blocks, the independent and uneven movement of each block may be inferred, and that would suggest a seismotectonic source for this relative sea-level drop. As it was not always possible to determine the inner edge of pebbly Unit D, two alternative measurements were taken: the height of Unit D's base, and the total height of the paleo-cliff.

The differences in altitude of the same geomarker along the studied sections must be related to more recent seismotectonic activity.

3.3. Paleoseismic indicators

Some specific features have been identified and interpreted as geological indicators of paleoseismicity. These are especially useful in the study of the seismic record in places like the Cope Basin, where the archaeological, historical and/or instrumental records of earthquakes are scarce. In the absence of other data, these geological indicators represent the only means of proposing a maximum intensity degree. The quantification of seismic intensity degree has been approached following the INQUA ESI-07 Scale (Environmental Seismic Intensity Scale; Guerrieri and Vittori, 2007), which only considers the earthquake environmental effects (EEEs) at inland and littoral locations (Fig. 9).

The ESI-07 Scale was created to fill the gap existing in sparsely populated areas where traditional damage-based macroseismic scales are difficult to apply. This scale has the further advantage of being applicable to different time-windows (recent or historical events), including paleo-earthquakes, when there are sufficient geological indicators (Guerrieri and Vittori, 2007). This macroseismic scale is structured in XII degrees and includes the record of primary and secondary effects. Primary effects are the expression of the seismogenic tectonic source (surface faulting and uplift/subsidence) and they only occur with intensity values ≥VIII. For their part, secondary effects are those generally induced by ground shaking, including ground cracks, slope movements, hydrological anomalies, anomalous waves/tsunamis, liquefactions and others (Fig. 9). These secondary effects can occur when intensity is ≥VI but they are significant again for intensities ≥VIII (Guerrieri and Vittori, 2007).

In our study case, probable paleoseismic evidence was found at points 7 to 11 (see Fig. 2 for location), all within the terrestrial sedimentary Unit C (see Fig. 4). The main features identified in this unit, which may be due to possible past seismic events, are related to liquefaction processes (Fig. 10):

1. Pervasive soft-sediment deformation structures. The fine facies (mud) of terrestrial Unit C, sometimes comprising its entire thickness (c. 1.2 m thick), are pervasively deformed by dm-thick

Please cite this article in press as: Bardají, T., et al., Coseismic vs. climatic factors in the record of relative sea level changes: an example from the Last Interglacials in SE Spain, Quaternary Science Reviews (2014), http://dx.doi.org/10.1016/j.quascirev.2014.10.005

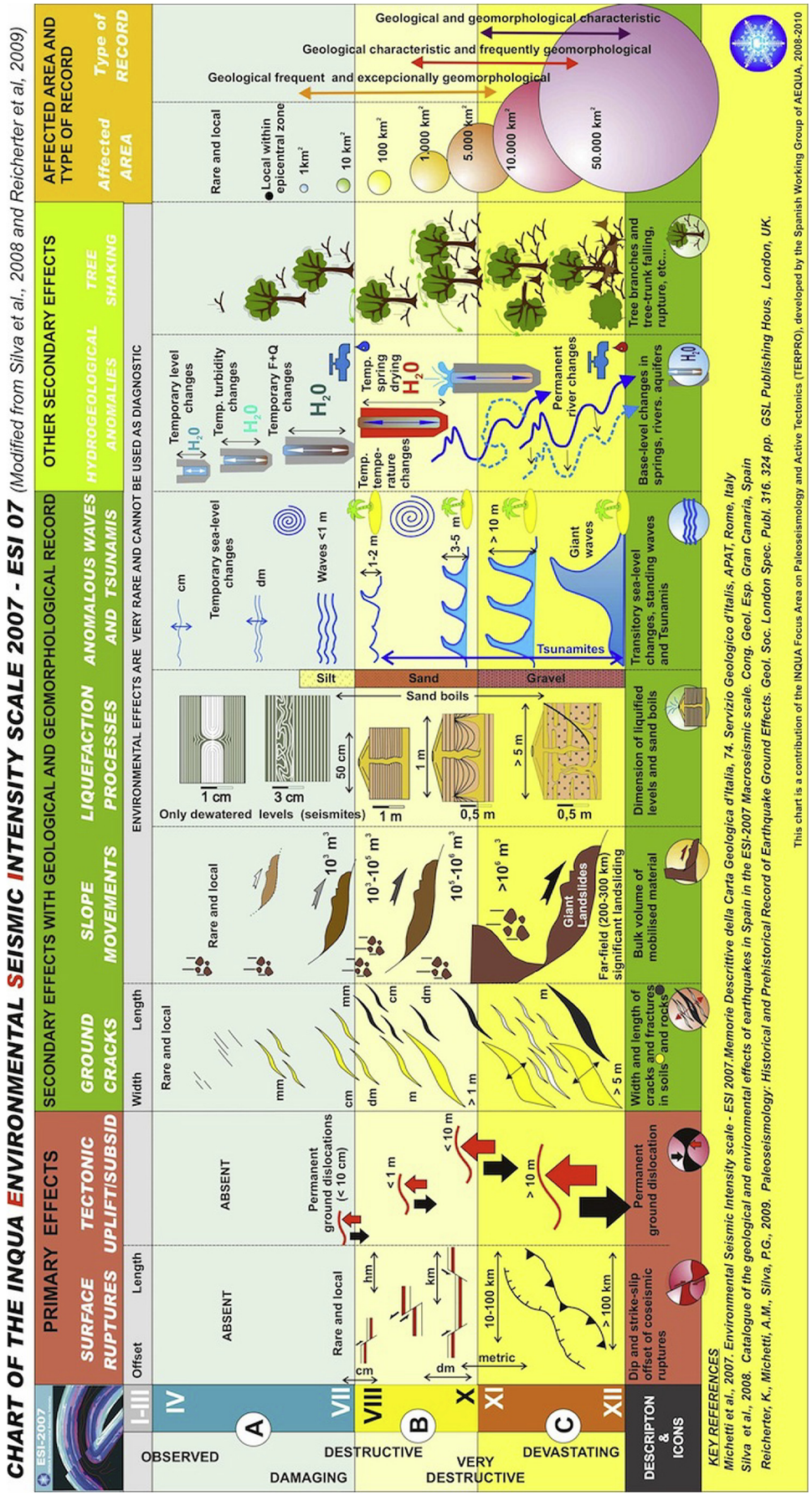

Fig. 9. Synoptic chart of ESI-2007 scale.

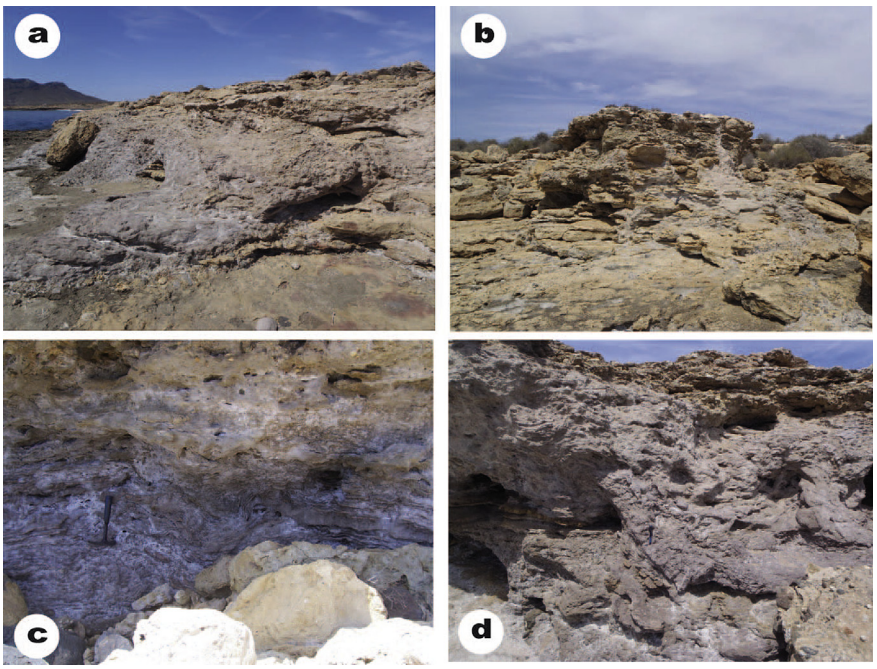

Fig. 10. Examples of the secondary effects of earthquakes identified within the studied sequence. a: slump-like structures (point 11); b: unconfined lateral spreading flow of Unit C over paleocliff and wave-cut "b" (point 7); c and d: Liquefaction features in fine sands and silts from Unit C (point 8).

convolute laminations and the development of complex pillar-dish arrangements, which may measure metres. The underlying well-cemented Units B and D show no signs of severe deformation, but at some points the overlying Unit D is noticeably cracked.

2. Flow or slump-like structures. In some cases, fine and coarse facies of Unit C, spread over the ancient cliff and above the former wave-cut bench "b", resembling limited mud-like flow bodies with visible wavy fronts spreading laterally over distances of a few metres. These flow or slump-like structures can be interpreted as a consequence of soft-sediment instability linked to near-surface liquefaction processes after the development of the paleo-cliff and associated wave-cut platform over which the sediments flowed. The formation of these erosive coastal features led to the water-saturated muddy sediments of Unit C to undergo limited flow in a laterally unconfined setting.

Paleoliquefaction features (1 and 2) identified in Unit C constitute a continuous horizon of deformation, visible for about 1 km along the coastline (points 11–7). Taking into account the thickness of the overlying Unit D (1.5–2 m), no overload processes can be considered to have produced the observed liquefaction features. Rather, seismically induced soft-sediment deformation needs to be regarded as the most probable trigger of the post-sedimentary liquefaction and overspread flow-like processes recorded in this unit.

3. Coastal uplift. There was a sudden relative sea-level drop between Unit D and the younger wave-cut bench "b" over which this unit underwent limited lateral overspread. This relative sea-level drop can be interpreted either as a sudden "eustatic" sea-level drop or as the result of coseismic uplift. The comparative altitudinal analyses carried out in Section 4.2 will provide important information for fully understanding the driving force behind this relative sea-level drop.

On the other hand, the differential uplift observed in the younger wave cut bench "b" can only be explained by later seismotectonic activity. The slip rate deduced from this uplift depends on the age of this wave cut bench, which will be discussed later.

4. Results

The analyses of the sedimentary facies of the defined key units, as well as their relative altitudinal disposition and particular morpho-sedimentary features allowed us to interpret the sedimentary evolution of this basin, especially as far as relative sea-level changes and their causes are concerned.

4.1. Interpretation of the sedimentary evolution

The morpho-sedimentary characteristics of the studied sequence allow the sea level history of this basin from at least the times of the Last Interglacials to be reconstructed. Assuming the chronology given in Section 2.2 and taking into account the sedimentological features and geomorphic assemblage of the described units, the history of sea-level changes can be summarized as follows:

(a) During MIS 7 (Unit B) sandy beaches developed in a slightly staircase arrangement into the former middle Pleistocene units and over a wide wave-cut platform (a in Fig. 4) carved into Plio-Pleistocene marine yellow calcarenites (Unit A). Unit B's sedimentary characteristics point to the occurrence of small-scale sea-level changes represented by the interbedded terrestrial layers within the foreshore/shoreface sandy beach sequence. These small-scale sea-level changes may not represent long time spans and could even be seasonal changes. However, the two different subunits identified, which showed marked differences in their progradation, could be interpreted as major sea-level oscillations within MIS 7.

(b) A subsequent sea-level drop triggered an important lowering of the fluvial base level, attested here by the strong erosional surface that separates Unit B from the terrestrial Unit C. The sandy beach levels at the top of this terrestrial unit could be interpreted as having been deposited in a terrestrial environment but close to the sea level, probably under rising sea-level conditions, at the end of MIS 6.

Please cite this article in press as: Bardají, T., et al., Coseismic vs. climatic factors in the record of relative sea level changes: an example from the Last Interglacials in SE Spain, Quaternary Science Reviews (2014), http://dx.doi.org/10.1016/j.quascirev.2014.10.005

(c) Overlying conglomeratic beaches (Unit D) developed on top of these units during a sea-level highstand higher than the former one. At least three different sea-level oscillations have been identified within this unit. The presence of *S. bubonius* and the lateral correlation with MIS 5e oolitihic sediments allow us to assume this age for this unit. Alluvial fan deposits found on top of the sequence in the northern part of the basin can be attributed to the Last Glacial. However we have no data to validate this chronology, and MIS 5b or 5d cannot be discarded.

(d) A subsequent sea-level drop is marked by the development of the cliff and wave-cut bench (b in Fig. 4) carved into the whole sedimentary sequence. This wave-cut bench represents a third highstand with a lower sea level than during the former MIS 5e unit. The age of this erosional feature depends on the age of the alluvial fans into which it cuts and implies a sufficiently stable high sea level for it to develop; therefore, it might date from MIS 5a/c or Holocene.

From the paleoseismic point of view, the soft-sediment sedimentary deformation and lateral overspread features of Unit C indicate that strong seismic shaking affected the zone after the excavation of the abovementioned wave-cut bench. In the absence of other reliable triggering-factors (e.g. sediment overloading), both sediment disturbance features indicate the occurrence of at least one significant paleoseismic event. Additionally, the spatial-height distribution of this wave-cut bench, ranging from 0 to 8 m a.m.s.l, points to the occurrence of surface folding, which is accommodated in the northern sector of the basin by subsequent faulting, since recorded steps of c. 2–2.5 m (i.e. points 4–5) can be hardly explained by folding on rocky-carved features such as occurs in La Galera–El Garrobillo sector. According to the macroseismic scale ESI-07 (Guerrieri and Vittori, 2007), the dimensions of the liquefaction features (Unit C) and the amount of differential uplift in the wave-cut bench correlate with a seismic intensity between VII and IX ESI-07 (see Fig. 9), which is much greater than the maximum intensity recorded instrumentally or historically in the Aguilas Arc (IV–V MSK; Mezcua, 1982).

4.2. Along-shore height distribution of key geomorphologic features

The analyses of the main sedimentary sequence along the selected points (see Fig. 2 for location) revealed interesting differences both in the morpho-sedimentary record and in the number of sea-level oscillations recorded, (Figs. 11–13). The first feature to be taken into account is the roughly constant amplitude between the inner edge of the upper conglomeratic unit (Unit D) and the shoreline angle of the post-MIS 5e wave-cut bench "b" (Table 1), which suggest a probable climatic (*eustatic*) cause for this sea-level drop between those two morpho-sedimentary features.

On the other hand, the height reached by all these units and especially by the younger wave-cut bench "b" was used to identify the occurrence of differential uplift among structural blocks (Table 1 and Fig. 14). These record apparent large wave-length folding in the southern sector of the basin, but short wave-length folding and subsequent faulting in its northern sector. Since the wave-cut bench analysed is an erosive rocky landform lacking any possible ductile behaviour, apparent folding results in subsequent ground ruptures which are mainly accommodated along the N120E fault system which governs the present landscape assemblage (Fig. 2).

5. Discussion

The morpho-sedimentary sequence analysed in this work provides new data to help interpret the nature of relative sea-level changes recorded since the MIS 7 in Cope Basin and propose a new geodynamic model for the area.

With respect to the relative sea-level changes, two components are involved and discussed: climatically induced sea-level changes and seismo-tectonic uplift.

Data about the relative elevation of sea level during MIS 7 are scarce and heterogeneous. Chappell and Shackleton (1986) suggest a position of 15 m b.s.l. whereas Roy and Boyd (1996) argue for 2–4 m a.s.l. in South Australia. Similar values of a sea-level at −18 to −9 m are given by Bard et al. (2002) on the basis of evidence from a stalagmite in the Argentarola cave (Italy). Dutton et al. (2009) use these values to analyse the amplitude and phasing of this interglacial in connection with northern hemisphere insolation. On the other hand, Murray-Wallace (2002) concludes that in that same area of Australia, interglacial sea levels have not differed more than 6 m from present values during the past eleven interglacials.

Pedoja et al. (2014) propose an uplifting scenario for coastal areas worldwide that results in a general staircase pattern for ancient strandlines related to regional geodynamics. They classify the different geodynamic scenarios on Earth as a function of their associated uplift rates, which range between 0.01 ± 0.01 and 1.47 ± 0.08 mm/yr. However, these authors fail to consider the effect of local tectonics and faults in the distribution of ancient coastlines.

A recent review paper on the Quaternary paleosea-level history of Spain (Zazo et al., 2013) suggests that the sea level during MIS 7 was not much lower (≤4 m) than at the peak of the Last Interglacial, MIS 5e. Thus, on the assumption that sealevel during MIS 7 was probably higher than present sealevel but below MIS 5e, Unit B may reasonably be attributed to MIS 7. Other data support this attribution: Unit B is always below Unit D and below oolitic (MIS 5e) dunes outcropping southwards, and both contains few specimens of *S. bubonius*.

The constant altitudinal differences between Unit D and the inner edge of wave cut "b" points to a climatically driven sea-level drop between both highstands rather than to any seismic origin. Assuming this climatic cause, the sea-level drop must be related to a more recent and lower sealevel position than MIS 5e or to a different highstand within MIS 5e. The age of the intermediate terrestrial unit (Unit G) found at points 2, 3, 4 and 6 (Figs. 11 and 12) is unknown, an incognita left unresolved by geomorphological mapping. Although previously assumed to be of the Last Glacial stage age (Bardají, 1999; Bardají et al., 2010), an MIS 5 age cannot be discarded.

As for the age of wave-cut bench "b", it seems clear that it was carved under stable highstand conditions, lower than peak MIS 5e. One of the hypotheses is that it could represent a younger highstand within MIS 5e. A synthesis of the Pleistocene marine terraces of the Spanish coast based on geomorphological mapping, morphosedimentary analysis, and faunal content, and supported by U-series dating (Zazo et al., 2003) pointed to the occurrence of up to three highstands during MIS 5e, between ~135 and ~117 ka. All three are characterized by warm "Senegalese" fauna (*S. bubonius*, *Cardita senegalensis*, *Conus testudinarius*, etc.). The oldest of these highstands were recorded in some of the east-facing coastal sectors of the Iberian Peninsula as prograding oolitic beach-coastal dune systems. The second is bio-siliciclastic and contains the most complete sedimentary and paleontological records, with a high number and variety of Senegalese species. Poorly sorted boulders embedded in a reddish matrix represent the third, most recent highstand. Bardají et al. (2009) proposed that the initially prevailing eastern winds turned into strong northerly winds by the end of MIS 5e, with increased storminess and runoff being the main cause of this facies change. On the other hand, these three highstands have been recognized in the general

Please cite this article in press as: Bardají, T., et al., Coseismic vs. climatic factors in the record of relative sea level changes: an example from the Last Interglacials in SE Spain, Quaternary Science Reviews (2014), http://dx.doi.org/10.1016/j.quascirev.2014.10.005

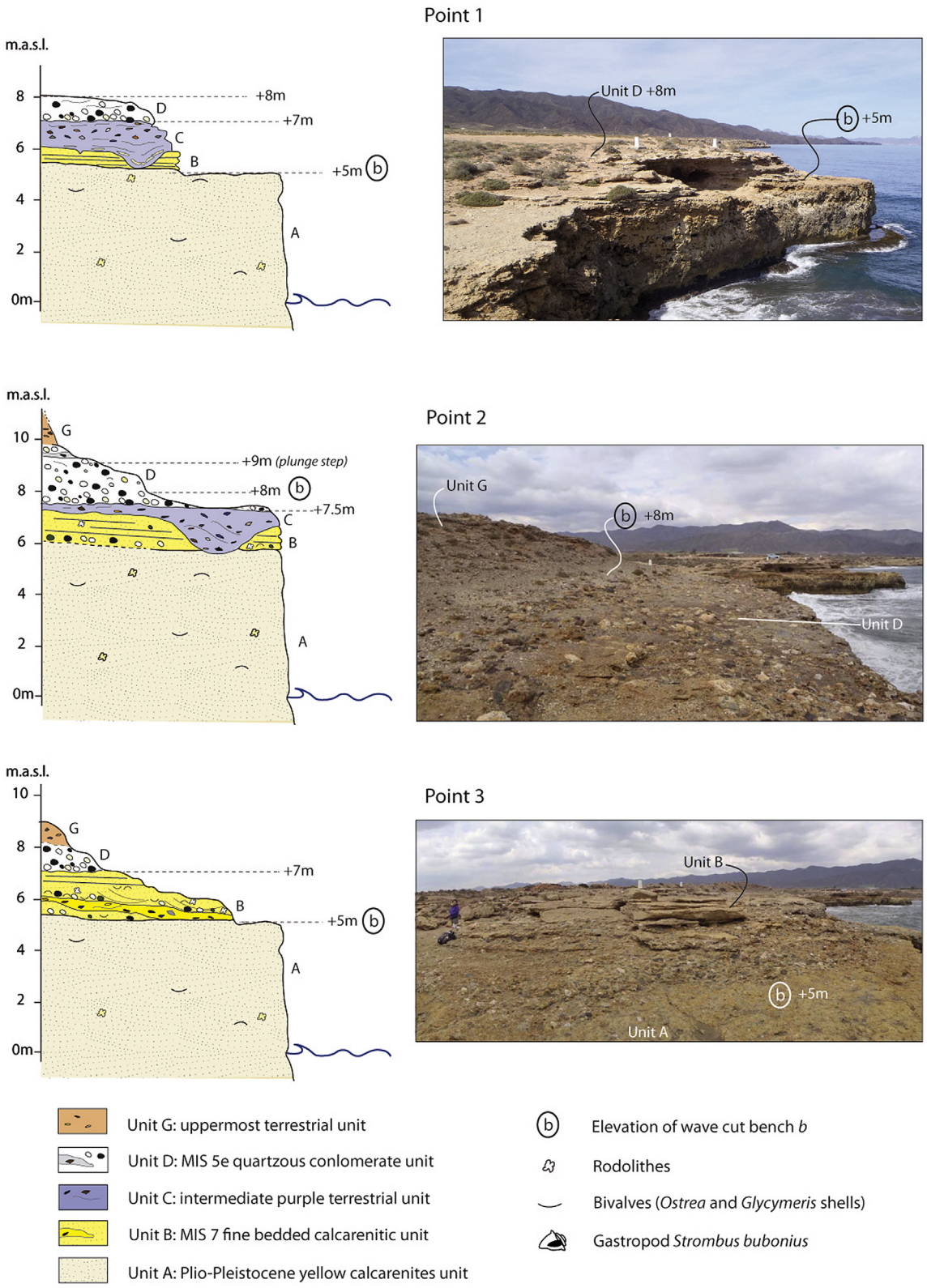

Fig. 11. Sedimentary sequence found at points 1, 2 and 3, (location in Fig. 2).

sea-level curve of the Mediterranean basin proposed by Hearty et al. (2007), based on data from Italy, Spain and Tunisia. Phreatic overgrowths in caves form the Island of Mallorca (Balearic Is.) record two highstands for MIS 5e (Tuccimei et al., 2006; Ginés et al., 2012), the ages and heights of which are consistent with those proposed by Hillaire Marcel et al. (1996) and Zazo et al. (2003) on the same island. We will take the values given by these authors of around +2.5 m and 120 ky for second MIS 5e highstand in Spanish western Mediterranean settings as our benchmark for calculating uplift rates.

Please cite this article in press as: Bardají, T., et al., Coseismic vs. climatic factors in the record of relative sea level changes: an example from the Last Interglacials in SE Spain, Quaternary Science Reviews (2014), http://dx.doi.org/10.1016/j.quascirev.2014.10.005

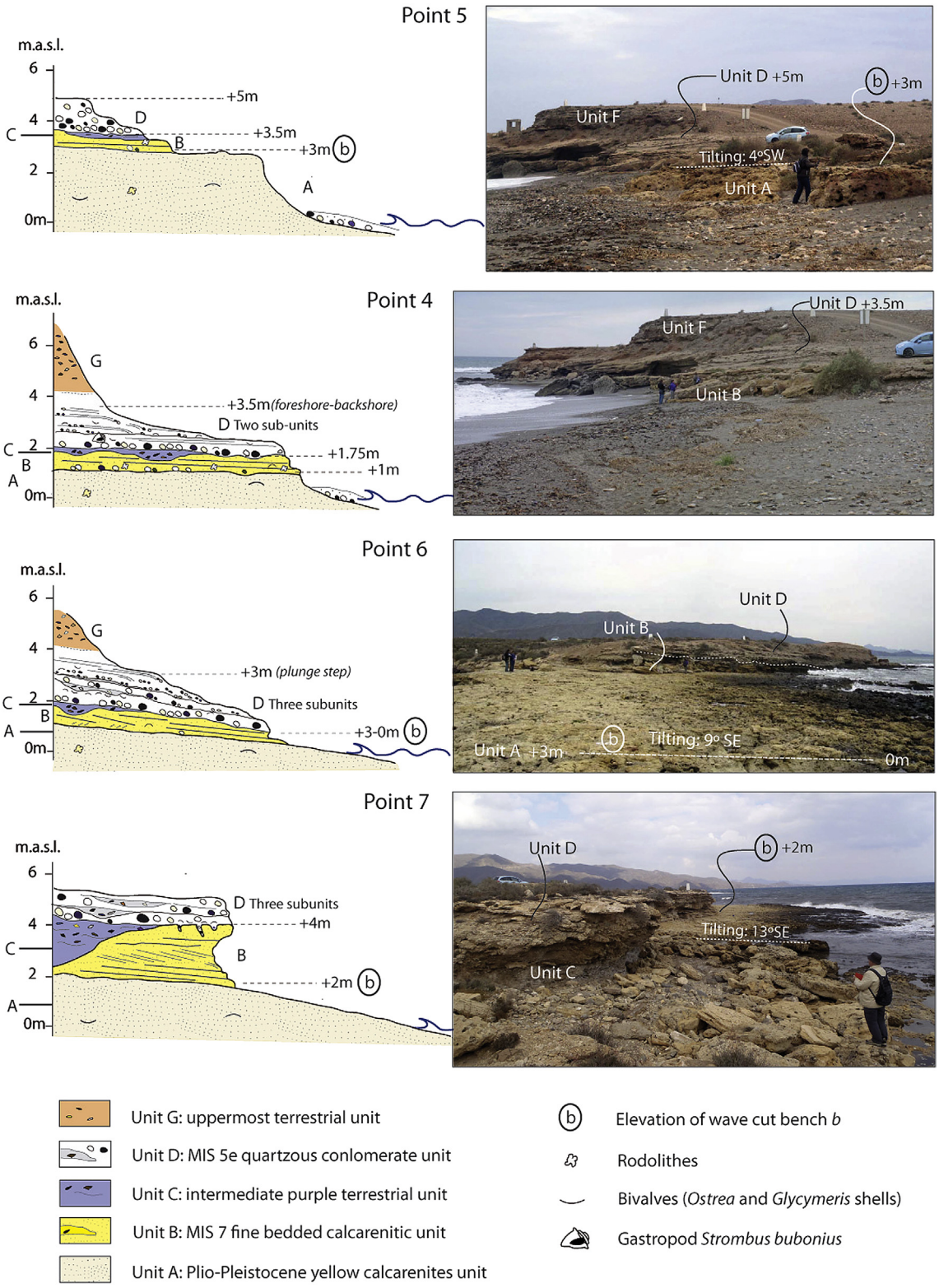

Fig. 12. Sedimentary sequence found at points 4, 5, 6 and 7, (location in Fig. 2).

A second hypothesis for the age of wave-cut bench "b" is that it could have been carved during MIS 5a (~80 ka). The sea level during this isotopic stage has also been much debated. Hearty and Kaufman (2000), Muhs (2002), and Hearty (2002) propose a relative highstand close or slightly above present sea level in Bahamas, as did Wehmiller et al. (2004) for the US Atlantic Coastal Plain. For the tectonically active coasts of Barbados, Schellmann and Radtke (2004) and Schellmann et al. (2004) suggested a sea level of about −20 m b.s.l. during MIS 5a, while in Haiti Dumas et al. (2006) proposed a sea level of −10 m b.s.l.

Please cite this article in press as: Bardají, T., et al., Coseismic vs. climatic factors in the record of relative sea level changes: an example from the Last Interglacials in SE Spain, Quaternary Science Reviews (2014), http://dx.doi.org/10.1016/j.quascirev.2014.10.005

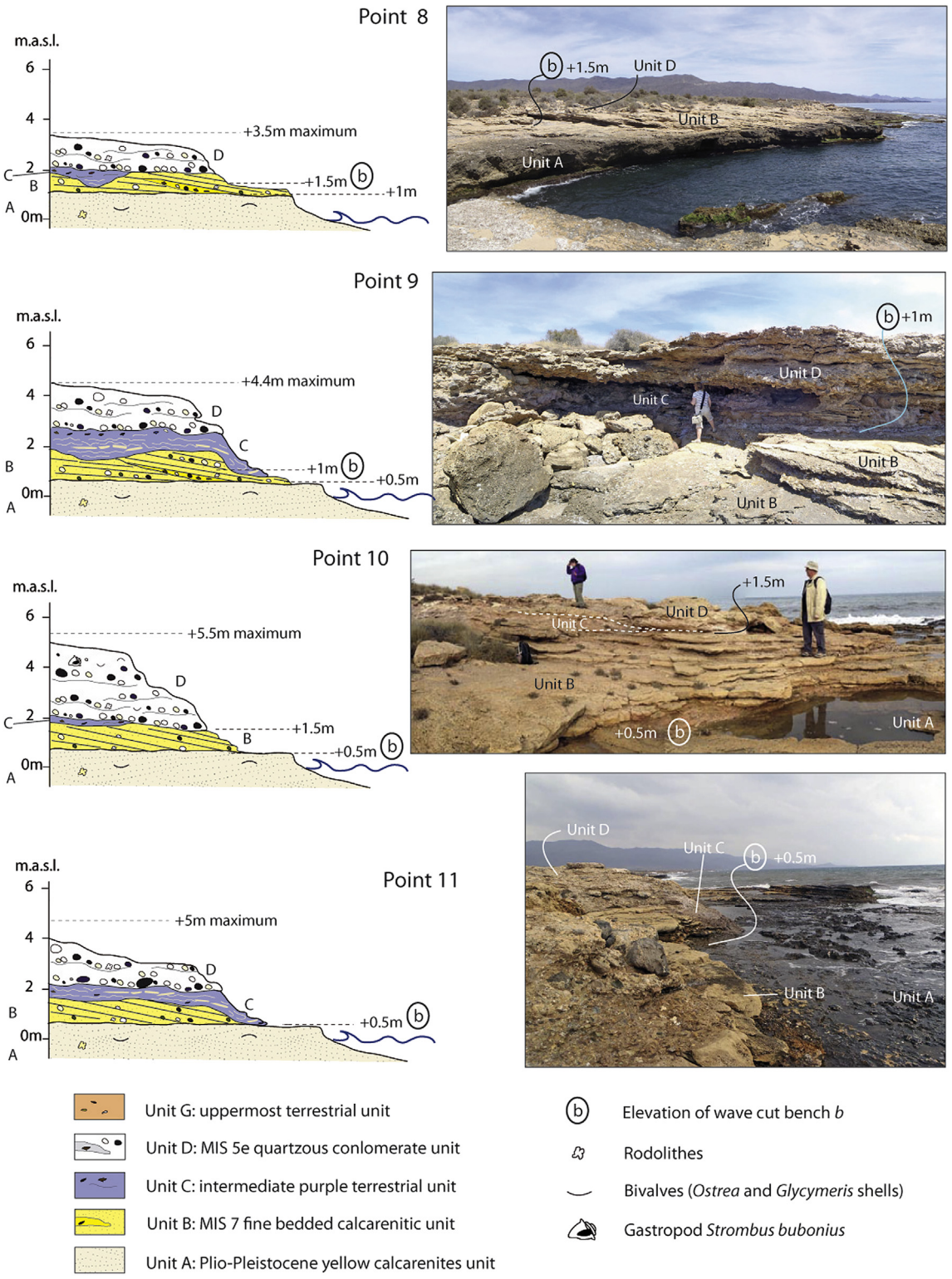

Fig. 13. Sedimentary sequence found at points 8 to 11, (location in Fig. 2).

The relative elevations of sea level after correcting the effects of glacio-isostasy (Stirling et al., 1998) point to eustatic sea-level values of up to −10 m b.s.l. at ~105 ka and ~80 ka. Therefore, reefs of this age could only outcrop above present sea level in areas undergoing uplift, such as Barbados and Haiti.

However, recent results based on U–Th dating on speleothem encrustations from coastal caves in Mallorca (Dorale et al., 2010) indicate a sea level during MIS 5a (81 ka) close to or slightly lower (+1.3–+1.9 m) than MIS 5e, quite in concordance with data from the Iberian Peninsula where a sea level lower than MIS 5e but pre-Holocene has also been detected above present sea level (Zazo et al., 2003, 2013).

In the absence of any precise chronology, faunal content, the distribution of morpho-sedimentary units and similarity with other

Table 1
Altitudinal measurements of reference geomorphologic features. Distance reference 0 m is Rambla Elena (See Fig. 2 for location of points).

Point	Distance (m)	Elevation of wave cut bench b (m)	Height of top cliff (m)	Inner edge of Unit D (m)	Amplitude of sea level change between Unit D and wave-cut bench b (m)
11	150	0.5	3	5	4.5
10	300	0.5	4.5	5.5	5
9	450	1	4.4	4.4	3.4
8	650	1.5	3.5	3.5	2
7	800	2	5	6	4
6	1200	3	5.5	–	–
6b	1250	0	2.5	–	–
4	1625	0	8	3.5	3.5
5	1700	3	5	7	4
3	2000	5	9	–	–
2	2200	8	12	–	–
1	2250	5	8	8	3

Last Interglacial sequences in Spain allow us to attribute a possible MIS 5 age to these units. However, we cannot be sure if wave-cut bench "b" was carved during a lower and younger highstand of MIS 5e or during MIS 5a.

Meanwhile, alluvial fans (Unit G) at the top of Unit D were clearly affected by the erosional event that carved wave-cut bench "b" and its associated paleocliff at points 2 and 3 (see Figs. 2 and 11). So if we assume a Last Glacial age for these alluvial fans, the wave-cut bench "b" must belong to the Holocene. Holocene sea-level has been reported to be at +0.8 m in nearby outcrops (Roquetas, Almería) at 5400 yr BP (Goy et al., 2003), while the prediction models based on the glacio-hydro-isostatic response of earth and ocean (Lambeck and Purcell, 2005) point to a sea-level position between −5 and −6 m (6000 yr BP) or between −0.5 and −0.75 m (2000 yr BP). As these are the only available field data close to the study area, we will take the values obtained at Roquetas as valid for the sole purpose of calculating uplift rates.

Assuming that this climatically driven (eustatic) wave-cut bench was created under high and steady sea-level conditions, it has three possible ages: second highstand of MIS 5e (2.5 m, 120 ka after Ginés et al., 2012), MIS 5a (1.3–1.9 m, 81 ka, after Dorale et al., 2010), and middle Holocene (0.8 m, 5400 yr BP after Goy et al., 2003). We have assumed these ages even though attempts to subdivide the Last Interglacial highstand exclusively on the basis of U/Th age have been largely inconclusive (Hearty et al., 2007) and Holocene sea level varies enormously from region to region.

As stated above, since we ascribe the unevenness of wave cut bench "b" to seismic activity, calculations of uplift rates are performed after taking the maximum altitude measured for this surface, that is +8 m at point 2 (see Fig. 2 for location). The resulting values give slip rates ranging from a minimum of 0.016 mm/yr (since MIS 5a) to a maximum of 0.15 mm/yr (since middle Holocene), whereas values obtained after assuming a MIS 5e age for the wave-cut bench lie between the two (0.020 mm/yr).

As for seismic activity in this basin and its role in the present distribution of marine terraces, we consider that the liquefaction structures found at points 6–11 are a clear indicator of seismic activity reaching intensity VII–VIII (ESI-07, see Fig. 9). In addition, permanent ground dislocations between 1 and 10 m (such as those presented here, Fig. 14) are related to ESI-07 VIII–IX intensities. These values are somewhat larger than intensities recorded by historic or instrumental data (see Section 2.2).

This altitudinal distribution of wave-cut bench "b" (Fig. 14) leads us to reconsider the previously mooted geodynamic model (Bardají, 1999; Bardají et al., 2010) which consisted of a southwards back-thrusting extension along the ancient Betic thrust-planes that might explain the opening of the basin on the one hand, and of the later differential movement of the faulted blocks that might explain the differential altitude on the other. This model was based on the depth of metamorphic Betic substratum and Pliocene units recorded at seven cores, as well as on the differential spatial-height distribution recorded by the early to middle Pleistocene marine terraces. However, as highlighted in Section 2.2, data on levelling lines (Giménez et al., 2000, 2009) and new research on tectonics and seismotectonics along the entire EBSZ (e.g. Silva et al., 2008; Martínez-Díaz et al., 2011; Alfaro et al., 2012) enable the structure of the Cope Basin to be compared with that of the present compressive front of the EBSZ at the Lower Segura blind fault. To be more precise, the height distribution of wave-cut bench "b" analysed in this study (Fig. 14 and top of Fig. 15) can be better explained by the occurrence of surface folding and subsequent faulting. Surface folding is related to blind thrusts affecting the underlying Plio-Quaternary series filling up the basin. For their part, vertical displacements of ca 2–2.5 m along N120E faults push-up the wave-cut bench to a height of +8 m a.m.s.l. over a distance of several hundred metres (Fig. 14). This zone may be considered a push-up structure linked to strike-slip reverse faulting on the compressive northern front of the basin against the metamorphic Betic substratum (Fig. 15).

However, the calculated slip rate values fall between the ranges of differential uplift rates evaluated by height-spatial analyses for the Betic Cordillera (Zazo et al., 2008) and those obtained by geodetic levelling within the Aguilas Arc (Giménez et al., 2000). The proposed geodynamic model supports these results.

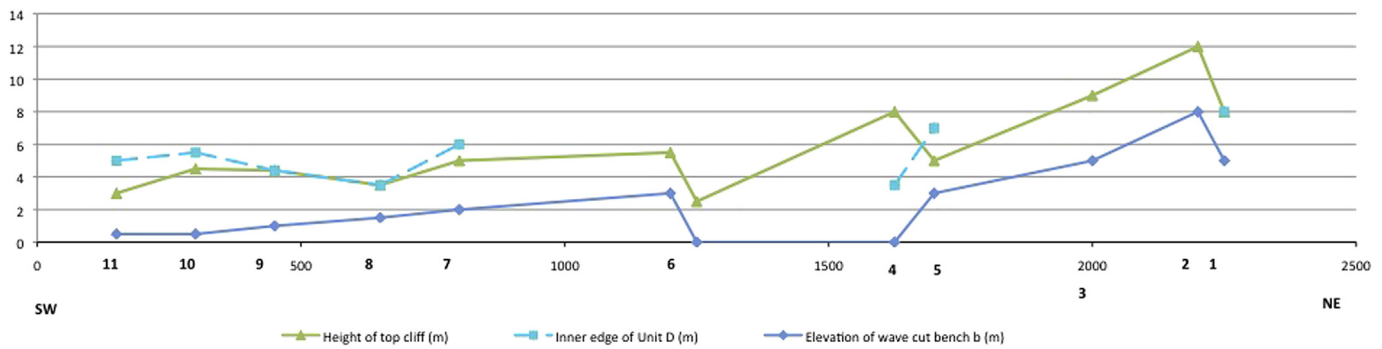

Fig. 14. Altitudinal distribution of the three selected key geomorphologic features along the coast studied. Distance is measured from Rambla Elena (see Fig. 2 for location). In green: Height of the present top of the cliff; in light blue: height of the inner edge of Unit D; in dark blue: height of the wave cut bench "b"; 1–11 m sections studied. (For interpretation of the references to colour in this figure legend, the reader is referred to the web version of this article.)

Please cite this article in press as: Bardají, T., et al., Coseismic vs. climatic factors in the record of relative sea level changes: an example from the Last Interglacials in SE Spain, Quaternary Science Reviews (2014), http://dx.doi.org/10.1016/j.quascirev.2014.10.005

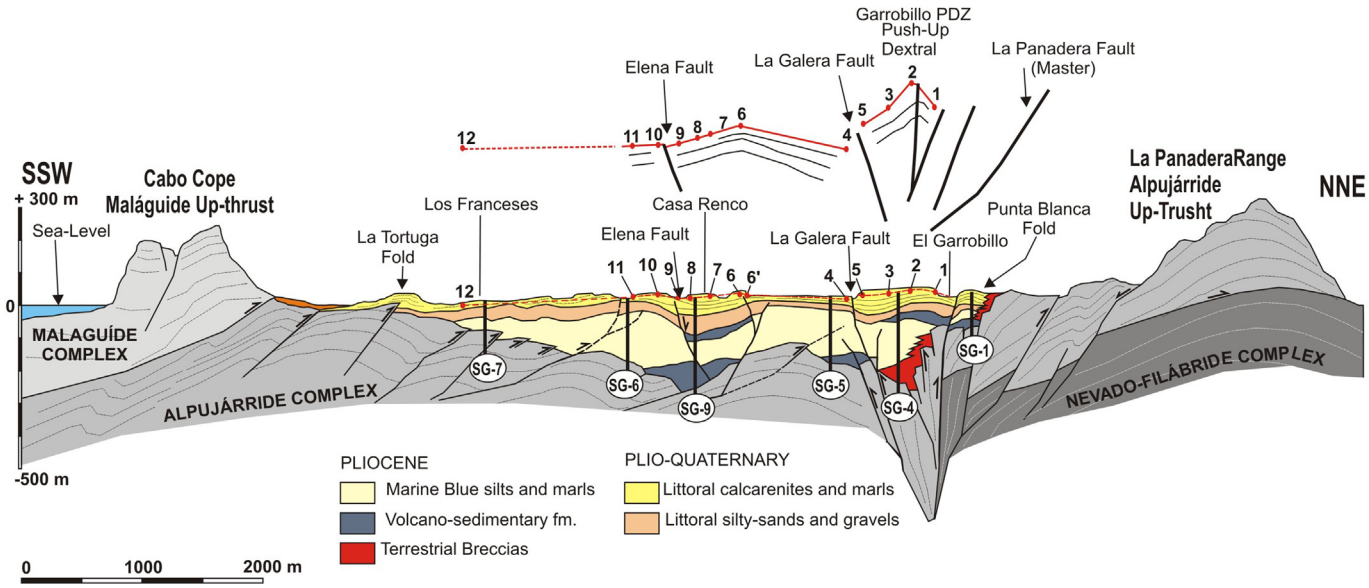

Fig. 15. Geodynamic model proposed for the Cope Basin. Altitudinal distribution of wave-cut bench on top. SG 1–7: location of drill cores; 1–11: selected points studied in this work.

6. Conclusions

The analysis of the MIS 7–MIS 5 marine terraces in Cope Basin (Murcia, SE Spain) allows the climatic (eustatic) and seismotectonic components in the record of sea-level changes to be differentiated.

Three main sedimentary units, two of littoral origin and an intermediate one of continental origin, compose the synthetic section; these three units are cut by a later paleocliff and associated wave-cut bench.

Geomorphologic disposition of these units points to a slightly lower sea level ($\leq$2 m) during MIS 7 than during MIS 5e in this coast. An important change in sedimentary style is also observed between MIS 7 and MIS 5e, from wide sandy beaches during MIS 7 to gravel beaches during MIS 5e. This change must be related to a change in marine weather and in sedimentary sources possible related to different climatic conditions and/or tectonic activity.

The detailed sedimentological and geomorphological analysis of these sedimentary units together with the altitudinal distribution of the wave-cut bench led us to separate the climatic (eustatic) signal from the seismotectonic one. Although the chronology is not certain, an averaged climatically induced sea-level drop of 3.5–4 m has been shown to occur between the upper sedimentary unit and the wave-cut bench. Assuming different chronological scenarios, this sea-level drop may have occurred within MIS 5e, between MIS 5e and MIS 5a, or between MIS 5e and mid-Holocene.

The existence of liquefaction structures attest seismic activity in an area where instrumental and/or historic record show no intensities higher than IV–V MSK, much lower than the VII–VIII or even IX ESI-07 obtained in this study.

Altitudinal investigation of the wave-cut bench gave uplift rates (slip rates) of between 0.016 and 0.15 mm/yr in this basin, assuming different ages for this surface (2nd highstand of MIS 5e, MIS 5a or mid-Holocene).

Finally, this research has made it possible to propose a different geodynamic model for the area, consisting of a push-up structure linked to strike-slip reverse faulting on the compressive northern front of the basin and the occurrence of surface folding and subsequent faulting. Blind faults may explain this surface folding and need to be taken into account in seismic hazard analyses. The seismic structures and unevenness of the wave-cut bench analysed in this work are the surface evidence of these hazardous blind faults.

Acknowledgements

Spanish Projects: CGL2012-33430, CGL2012-37581-CO2-01, CGL2013-42847-R and ACI-2009-1037. This work is a contribution of the Spanish Working Group of IGCP Project 588, INQUA CMP WG on Long Term Sea-level Changes, INQUA TERPRO Project 1299 (EEE Metrics) and Research Group UCM 910198 (Paleoclimatology and Global Change). We thank the support given by Loreto Antón in the plotting of IGN seismic data and also to the anonymous referees for their advice and suggestions, which have really improved this paper.

References

Alfaro, P., Bartolomé, R., Borque, J.M., Estévez, A., García-Mayordomo, J., García-Tortosa, F.J., Gil, A.J., Gràcia, E., Lo Iacono, C., Perea, H., 2012. The Bajo Segura Fault Zone: active blind thrusting in the Eastern Betic Cordillera (SE Spain). J. Iber. Geol. 38 (1), 271–284.

Bahrouni, N., Bouaziz, S., Soumaya, A., Be Ayed, N., Attafi, K., Holua, Y., El Ghali, A., Rebai, N., 2014. Neotectonic and seismotectonic investigation of seismically active regions in Tunisia: a multidisciplinary approach. J. Seismol. 18, 235–256.

Bard, E., Antonioli, F., Silenzi, S., 2002. Sea-level during the penultimate interglacial period based on a submerged stalagmite from Argentarola Cave (Italy). Earth and Planetary Science Letters 196, 135–146.

Bardají, T., Civis, J., Dabrio, C.J., Goy, J.L., Somoza, L., Zazo, C., 1986. Geomorfología y estratigrafía de las secuencias marinas y continentales cuaternarias de la Cuenca de Cope (Murcia, España). In: López, F., Thornes, J.B. (Eds.), Estudios sobre Geomorfología del Sur de España. Universidad de Murcia, pp. 11–16.

Bardají, T., 1999. Evolución Geomorfológica durante el Cuaternario de las Cuencas Neógenas litorales del Sur de Murcia y Norte de Almería (PhD thesis). Universidad Complutense de Madrid, 492 pp.

Bardají, T., Goy, J.L., Mörner, N.A., Zazo, C., Silva, P.G., Somoza, L., Dabrio, C.J., Baena, J., 1995. Towards a Plio-Pleistocene chronostratigraphy in Eastern Betic Basins. Geodin. Acta 8 (2), 112–126.

Bardají, T., Goy, J.L., Zazo, C., Hillaire-Marcel, C., Dabrio, C.J., Cabero, A., Ghaleb, B., Silva, P.G., Lario, J., 2009. Sea level and climate changes during OIS 5e in the Western Mediterranean. Geomorphology 104, 22–37.

Bardají, T., Silva, P.G., Zazo, C., Goy, J.L., 2010. Cartografía y memoria del Cuaternario, Geomorfología y Procesoso Activos. In: Mapa Geológico Nacional, Serie MAGNA, 3ª Serie. IGME.

Bousquet, Ph, 1979. Quaternary strike-slip faults in southeastern Spain. Tectonophysics 52, 277–286.

Chappell, J., Shackleton, N.J., 1986. Oxygen isotopes and sea level. Nature 324, 137–140.

Please cite this article in press as: Bardají, T., et al., Coseismic vs. climatic factors in the record of relative sea level changes: an example from the Last Interglacials in SE Spain, Quaternary Science Reviews (2014), http://dx.doi.org/10.1016/j.quascirev.2014.10.005

Coppier, G., Griveaud, P., Larouziere, F.D., Montenat, Ch., Ott d'Estevou, Ph., 1989. Example of Neogene tectonic indentation in the Eastern Betic Cordilleras: the Arc of Aguilas (Southeastern Spain). Geodin. Acta 3, 37–51.

Cuci, L., Tertuliani, A., 2010. The Capo Vaticano (Calabria) coastal terraces and the 1905 M7 earthquake: the geomorphological signature of regional uplift and coseismic slip in southern Italy. Terra Nova 22, 378–389. http://dx.doi.org/10.1111/j.1365-3121.2010.00961.x.

Dabrio, C.J., Goy, J.L., Zazo, C., 1985. A model of conglomeratic beaches in tectonically active areas (Late Pleistocene-Actual, Almería, Spain). In: 6th IAS European Regional Meeting of Sedimentology, Lleida, Spain, pp. 104–107.

Dabrio, C.J., Zazo, C., Goy, J.L., Santiesteban, C., Bardají, T., Somoza, L., Baena, J., Silva, P.G., 1991. Neogene and Quaternary fan-delta deposits in southeastern Spain. Cuad. Geol. Iber. 15, 327–400.

Dabrio, C.J., Zazo, C., Cabero, A., Goy, J.L., Bardají, T., Hillaire-Marcel, C., González-Delgado, J.A., Lario, J., Silva, P.G., Borja, F., García-Blázquez, A.M., 2011. Millennial/submillennial-scale sea-level fluctuations in Western Mediterranean during the second highstand of MIS 5e. Quat. Sci. Rev. 30, 335–346.

Dorale, J.A., Onac, B.P., Fornós, J.J., Ginés, J., Ginés, A., Tuccimei, P., Peate, D.W., 2010. Sea-level 81,000 years ago in Mallorca. Science 327, 860–863.

Dumas, B., Hoang, C.T., Raffy, J., 2006. Record of MIS 5 sea-level highstands based on U/The dated coral terraces of Haiti. Quat. Int. 145–146, 106–118.

Dutton, A., Lambeck, K., 2012. Ice volume and sea level during the Last Interglacial. Science 337, 216–219.

Dutton, A., Bard, E., Antonioli, F., Esat, T.M., Lambeck, K., McCulloch, M.T., 2009. Phasing and amplitude of se-level and climate change during the penultimate interglacial. Nat. Geosci. 2, 355–359.

Ferranti, L., Monaco, C., Antonioli, F., Maschio, L., Kershaw, S., Verrubbi, V., 2007. The contribution of regional uplift and coseismic slip to the vertical crustal motion in the Messina Straits, southern Italy: evidence from raised Late Holocene shorelines. J. Geophys. Res. 112, B06401. http://dx.doi.org/10.1029/2006JB004473.

Giménez, J., Suriñach, E., Goula, X., 2000. Quantification of vertical movements in the eastern Betics (Spain) by comparing levelling data. Tectonophysics 317, 237–258.

Giménez, J., Borque, M.J., Gil, A., Alfaro, P., Estévez, A., Suriñach, E., 2009. Comparison of long-term and short-term uplift rates along an active blind reverse fault zone (Bajo Segura, SE Spain). Stud. Geophys. Geod. 53, 81–98.

Ginés, J., Ginés, A., Fornós, J.J., Tuccimei, P., Onac, B.P., Gràcia, F., 2012. Phreatic Overgrowths on speleothems (POS) from Mallorca, Spain: updating forty years of research. In: Ginés, A., Ginés, J., Gómez-Pujol, L., Onac, B.P., Fornós, J.J. (Eds.), Mallorca: a Mediterranean Benchmark for Quaternary Studies. Mon. Soc. Hist. Nat. Balears 18, 111–146.

Goy, J.L., Somoza, L., Bardají, T., Zazo, C., 1987. Shoreline mapping models in areas with different morphosedimentary behaviour (Almeria–Murcia–Alicante, Spain). Late Quaternary Sea-level Changes in Spain. Trabajos Sobre Neogeno-Cuaternario 10, 35–47.

Goy, J.L., Zazo, C., Somoza, L., Dabrio, C.J., 1990. Evolución paleogeográfica de la Depresión de Elche-Cuenca del Bajo Segura (España) durante el Pleistoceno. Estud. Geol. 46, 237–244.

Goy, J.L., Zazo, C., Bardají, T., Somoza, L., Causse, C., Hillaire-Marcel, C., 1993. Eléments d'une chronostratigraphie du Tyrrhénien des régions d'Alicante-Murcia, Sud-est de l'Espagne. Geodin. Acta 6-2, 103–119.

Griveaud, Ph., 1989. Etude Géologique du secteur d'Aguilas (Sud-est de l'Espagne): Exemple de poinçonnement néogène dans la zone Bétique interne oriental (PhD thesis). Univ. Claude Bernard, Lyon 1, France, 198 pp.

Guerrieri, L., Vittori, E., 2007. Environmental Seismic Intensity Scale 2007—ESI 2007. In: Memorie Descrittive della Carta Geologica d'Italia, vol. 74. Servizio Geologico d'Italia–Dipartimento Difesa del Suolo, APAT, Roma, Italy, 54 pp.

Hearty, P.J., 2002. Revision of the late Pleistocene stratigraphy of Bermuda. Sediment. Geol. 153, 1–21.

Hearty, P.J., Kaufman, D.S., 2000. Whole-rock aminostratigraphy and Quaternary sea level history of the Bahamas. Quat. Res. 54, 163–173.

Hearty, P.J., Hollin, J.T., Neumann, A.C., O'Leary, M.J., McCulloch, M., 2007. Global sea-level fluctuations during the Last Interglaciation (MIS 5e). Quat. Sci. Rev. 26, 2090–2112.

Hillaire Marcel, Cl, Gariépy, C., Ghaleb, B., Goy, J.L., Zazo, C., Cuerda, J., 1996. U-Series measurements in Tyrrhenian deposits from Mallorca. Further evidence for two Last Interglacial high sea levels in the Balearic Islands. Quat. Sci. Rev. 15, 53–62.

IDERM, 2014. Infraestructura de Datos Espaciales de la Región de Murcia. Available from: http://iderm.imida.es/iderm/ (accessed 15.03.14.).

IGN, 2014. Instituto Geográfico Nacional; Catálogo de terremotos [Online]. Available from: http://www.ign.es/ign/layoutIn/sismoFormularioCatalogo.do (accessed 12.07.13.).

Kopp, R.E., Simons, F.J., Mitrovica, J.X., Maloof, A.C., Oppenheimer, M., 2009. Probabilistic assessment of sea level during the last interglacial stage. Nature 462, 863–867.

Lambeck, K., Purcell, A., 2005. Sea-level change in the Mediterranean Sea since the LGM: model predictions for tectonically stable areas. Quaternary Science Reviews 24, 1969–1988.

Larouziere, F.D., Bolze, J., Bordet, P., Hernández, J., Montenat, Ch., Ott d'Estevou, Ph., 1988. The Betic segment of the trans-Albroan shear zone during the Late Miocene. Tectonophysics 152, 41–52.

Martínez-Díaz, J.J., 2002. Stress field variety related to fault interaction in a reverse oblique-slip fault: the Alhama de Murcia Fault, Betic Cordillera, Spain. Tectonophysics 356, 291–305.

Martínez-Díaz, J.J., Rodríguez-Pascua, M.A., Pérez López, R., García Mayordomo, J., Giner Robles, J., Martín-González, F., Rodríguez Peces, M., Álvarez Gómez, J.A., Insua Arévalo, J.M., 2011. Informe Geológico Preliminar del Terremoto de Lorca del 11 de mayo del año 2011 (5.1 Mw) . Instituto Geológico y Minero Internal Report.

Maouche, S., Meghraoui, M., Morhange, C., Belabbes, S., Bouhadad, Y., Haddoum, H., 2011. Active coastal thrusting and folding, and uplift rate of the Sahel Anticline and Zemmouri earthquake area (Tell Atlas, Algeria). Tectonophysics 509, 69–80.

Melnick, D., Cisternas, M., Moreno, M., Norambuena, R., 2012. Estimating coseismic coastal uplift with an intertidal mussel: calibration for the 2010 Maule Chile earthquake (Mw = 8.8). Quat. Sci. Rev. 42, 29–42.

Meltzner, A.J., Sieh, K., Abrams, M., Agnew, D.C., Hudnut, K.W., Avouac, J.P., Natawidjaja, D.H., 2006. Uplift and subsidence associated with the great Aceh-Andaman earthquake of 2004. J. Geophys. Res. 111, B02407. http://dx.doi.org/10.1029/2005JB003891.

Mezcua, J., 1982. Catálogo General de Isosistas de la Península Ibérica. Instituto Geográfico Nacional. Pub. 202, 319 pp.

Montenat, Ch., Ott D'Estevou, Ph., Masse, P., 1987. Tectonic-sedimentary characters of the Betic Neogene basins evolving in a crustal transcurrent shear zone (SE Spain). Cent. Rech. Explor. Prod. Elf Aquitaine 11, 1–22.

Morelli, A., Barrier, E., 2004. Geodynamic Map of the Mediterranean. Sheet 2: Seismicity and Tectonics. Commission for the Geological Map of the World.

Muhs, D.R., 2002. Evidence for the timing and duration of the Last Interglacial period from high-precision uranium-series ages of corals on tectonically stable coastlines. Quat. Res. 58, 36–40.

Murray-Wallace, C., 2002. Pleistocene coastal stratigraphy, sea-level highstands and neotectonism of the southern Australian passive continental margin – a review. J. Quat. Sci. 17, 469–489.

Nelson, A.R., Shennan, I., Long, A.J., 1996. Identifying coseismic subsidence in tidal-wetland stratigraphic sequences at the Cascadia subduction zone of western North America. Journal of Geophysical Research 101, 6115–6135.

Ortlieb, L., Barrientos, S., Guzman, N., 1996a. Coseismic coastal uplift and coralline algae record in Northern Chile: the 1995 Antofagasta earthquake case. Quat. Sci. Rev. 15 (8), 949–960.

Ortlieb, L., Zazo, C., Goy, J.L., Hillaire-Marcel, Cl., Ghaleb, B., Cournoyer, L., 1996b. Coastal deformation and sea-level changes in the northern Chile subduction area (23°S) during the last 330 ky. Quat. Sci. Rev. 15 (8–9), 819–831.

Ott d'Estevou, Ph., Montenat, Ch., 1985. Evolution structurale de la zone bétique orientale (Espagne) du Tortonien a l'Holocène. C.R. Acad. Sci. Paris 300 (Sèrie II, n. 8), 363–368.

Ozawa, S., Nishimura, T., Suito, H., Kobayashi, T., Tobita, M., Imakiire, T., 2011. Coseismic and postseismic slip of the 2011 magnitude-9 Tohoku-Oki earthquake. Nature 475, 373–376.

Pedoja, K., Husson, L., Regard, V., Cobbold, P.R., Ostanciaux, E., Johnson, M.E., Kershaw, S., Saillard, M., Martinod, J., Furgerot, L., Weill, P., Delcaillau, B., 2011. Relative sea-level fall since the last interglacial stage: are coasts uplifting worldwide? Earth Sci. Rev. 108, 1–15.

Pedoja, K., Husson, L., Johnson, M.E., Melnick, D., Witt, C., Pochat, S., Nexer, M., Delcaillau, B., Pinegina, T., Poprawski, Y., Authemayou, C., Elliot, M., Regard, V., Garestier, F., 2014. Coastal staircase sequences reflecting sea-level oscillations and tectonic uplift during the Quaternary and Neogene. Earth Sci. Rev. 132, 13–38.

Reicherter, K., Michetti, A.M., Silva, P.G., 2009. Palaeoseismology: historical and prehistorical records of earthquake ground effects for seismic hazard assessment. Geol. Soc. London, Spec. Publ. 316, pp. 1–10. London, UK.

Plafker, G., 1969. Tectonics of the March 27, 1964. In: Alaska earthquake: U.S. Geological Survey Professional Paper, vol. 543-I, p. 74.

Rodríguez-Vidal, J., Cáceres, L.M., Finlayson, J.C., Gracia, F.J., Martínez-Aguirre, A., 2004. Neotectonics and shoreline history of the Rock of Gibraltar, southern Iberia. Quat. Sci. Rev. 23, 2017–2029.

Roy, P.S., Boyd, R., 1996. Quaternary Geology of a Tectonically Stable, Wave Dominated, Sediment-deficient Margin, Southeast Australia. IGCP Project 367, Field Guide to the Central South Wales Coast. New South Wales Geological Survey, Sydney, 174 p.

Schellmann, G., Radtke, U., 2004. A revised morpho- and chronostratigraphy of the Late and Middle Pleistocene coral reef terraces on southern Barbados (West Indies). Earth Sci. Rev. 64, 157–187.

Schellmann, G., Radtke, U., Potter, E.-K., Esat, T.M., McCulloch, M.T., 2004. Comparison of ESR and TIMS U/Thdating of marine isotope stage (MIS) 5e, 5c, and 5a coral from Barbados-implications for palaeo sea-level changes in the Caribbean. Quat. Int. 120, 41–50.

Siddall, M., Chappell, J., Potter, E.-K., 2006. Eustatic sea level during past interglacials. In: Sirocko, F., Claussen, M., Sanchez Goñi, M.F., Litt, T. (Eds.), The Climate of Past Interglacials. Elsevier, Amsterdam, pp. 75–92.

Silva, P.G., 1994. Evolución geodinámica de la Depresión del Guadalentín desde el Mioceno Superior hasta la actualidad: Neotectónica y Geomorfología (PhD thesis). Universidad Complutense de Madrid, Spain, p. 642.

Silva, P.G., Goy, J.L., Somoza, L., Zazo, C., Bardají, T., 1993. Landscape response to strike-slip faulting linked to collisional settings: Quaternary tectonics and basin formation in the Eastern Betics, southeastern Spain. Tectonophysics 224, 289–303.

Silva, P.G., Goy, J.L., Zazo, C., Bardají, T., 2003. Fault generated mountain fronts in southeast Spain: geomorphologic assessment of tectonic and seismic activity. Geomorphology 250, 203–226.

Silva, P.G., Rodríguez-Pascua, M., Pérez-López, R., Bardají, T., Lario, J., Alfaro, J.J., Martínez-Díaz, J.J., Reicherter, K., Giménez, J., Giner, J., Azañón, J.M., Goy, J.L., Zazo, C., 2008. Catalogación de los efectos geológicos y ambientales de los terremotos en España en la Escala ESI-2007 y su aplicación a los estudios paleosismológicos. Geotemas 10, 318.

Please cite this article in press as: Bardají, T., et al., Coseismic vs. climatic factors in the record of relative sea level changes: an example from the Last Interglacials in SE Spain, Quaternary Science Reviews (2014), http://dx.doi.org/10.1016/j.quascirev.2014.10.005

Somoza, L., 1989. Estudio del Cuaternario litoral entre Cabo de Palos y Guardamar (Murcia–Alicante). Las variaciones del nivel del mar en relación con el contexto geodinámico (PhD thesis). Universidad Complutense de Madrid. Facultad de Geología, 325 pp.

Stirling, C.H., Esat, T.M., Lambeck, K., McCulloch, M.T., 1998. Timing and duration of the last Interglacial: evidence for a restricted interval of widespread coral reef growth. Earth Planet. Sci. Lett. 160, 745–762.

Tuccimei, P., Ginés, J., Delitala, C., Pazzelli, L., Taddeucci, A., Clamor, B., Fornós, J.J., Ginés, A., 2006. Last Interglacial sea-level changes in Mallorca island (Western Mediterranean). High precision U-series data from phreatic overgrowths on speleothems. Z. Geomorphol. 50, 1–21.

Tuccimei, P., Onac, B.P., Dorale, J.A., Ginés, J., Fornós, J.J., Ginés, A., Spada, G., Riggieri, G., Muceda, M., 2012. Decoding the last Interglacial sea level variations in the western Mediterranean using speleothem encrustations from coastal caves in Mallorca and Sardinia: a field data – model comparison. Quat. Int. 262, 56–64.

Wehmiller, J.F., Simmons, K.R., Cheng, H., Edwards, R.L., Martin-McNaughton, J., York, L.L., Krantz, D.E., Shen, C.-C., 2004. Uranium-series coral age from the US Atlantic Coastal plain. The "80 ka problem" revisited. Quat. Int. 120, 3–14.

Weijermars, R., 1987. The Palomares brittle-ductile shear zone of southern Spain. J. Struct. Geol. 9, 139–157.

Zazo, C., Bardají, T., Dabrio, C.J., Goy, J.L., Hillaire-Marcel, C., 1998. Record of Late Pliocene and Quaternary sea-level changes in coastal settings, southeast Spain. In: Meléndez-Hevia, A., Soria, A.R. (Eds.), 15th International Congress of Sedimentology, Alicante, Spain. ITGE, Madrid, pp. 151–169.

Zazo, C., Goy, J.L., Dabrio, C.J., Bardají, T., Hillaire-Marcel, C., Ghaleb, B., González-Delgado, A., Soler, V., 2003. Pleistocene raised marine terraces of the Spanish Mediterranean and Atlantic coasts: records of coastal uplift, sea-level high-stands and climate changes. Mar. Geol. 194, 103–133.

Zazo, C., Goy, J.L., Dabrio, C.J., Lario, J., González-Delgado, A., Bardají, T., Hillaire-Marcel, C., Cabero, A., Ghaleb, B., Borja, F., Silva, P.G., Roquero, E., Soler, V., 2013. Retracing the Quaternary history of sea-level changes in the Spanish Mediterranean-Atlantic coasts: geomorphological and sedimentological approach. Geomorphology 196, 36–49.

Please cite this article in press as: Bardají, T., et al., Coseismic vs. climatic factors in the record of relative sea level changes: an example from the Last Interglacials in SE Spain, Quaternary Science Reviews (2014), http://dx.doi.org/10.1016/j.quascirev.2014.10.005